PRWG-96-1

Utah State University

Logan, Utah 84321

# Studies to Develop and Investigate an Inverse Formulation for Numerically Solving Three-dimensional Free Surface Potential Fluid Flows

Utah Water Research Laboratory/College of Engineering
By Roland W. Jeppson
May 1972

This research was carried out under the Naval Ship Systems Command General Hydromechanics Research Program Subprogram SR 009 01 01, administered by the Naval Ship Research and Development Center under Contract N00014-67-A-0220-0003



44

Unclassified

Security Classification

**DOCUMENT CONTROL DATA - R & D**

(Security classification of title, body of abstract and indexing annotation must be entered when the overall report is classified)

| | |
|---|---|
| 1. ORIGINATING ACTIVITY (Corporate author)<br>Utah Water Research Laboratory<br>Utah State University<br>Logan, Utah 84321 | 2a. REPORT SECURITY CLASSIFICATION<br>Unclassified<br>2b. GROUP |

3. REPORT TITLE STUDIES TO DEVELOP AND INVESTIGATE AN INVERSE FORMULATION FOR NUMERICALLY SOLVING THREE-DIMENSIONAL FREE SURFACE POTENTIAL FLUID FLOWS

4. DESCRIPTIVE NOTES (Type of report and inclusive dates)

5. AUTHOR(S) (First name, middle initial, last name)
Roland W. Jeppson

| | | |
|---|---|---|
| 6. REPORT DATE<br>March 1972 | 7a. TOTAL NO. OF PAGES<br>37 | 7b. NO. OF REFS<br>20 |
| 8a. CONTRACT OR GRANT NO<br>N00014-67-A-0220-0003<br>b. PROJECT NO<br>SR 009 01 01<br>c. Naval Ship Systems Command<br>d. General Hydromechanics Research Program | 9a. ORIGINATOR'S REPORT NUMBER(S)<br>PRWG96-1<br>9b. OTHER REPORT NO(S) (Any other numbers that may be assigned this report) | |

10. DISTRIBUTION STATEMENT
This document has been approved for public release and sale; its distribution is unlimited.

| | |
|---|---|
| 11. SUPPLEMENTARY NOTES | 12. SPONSORING MILITARY ACTIVITY<br>Naval Ship Research & Development Center, Washington, D.C. 20034 |

13. ABSTRACT

An inverse formulation is developed for solving three-dimensional potential fluid flows which considers the magnitudes of the cartesian coordinates x, y, and z as the dependent variables in the space defined by (i.e. the independent variables) the potential function and two mutually orthogonal stream surface functions whose intersection defines the physical space streamlines. This formulation reverses the usual role of the variables. In this inverse space irregular boundaries, with unknown position in the physical space, such as free surfaces become plane boundaries, and the space of most potential flow problems is a parallelepiped.

The basic partial differential equations resulting from this formulation are nonlinear and three in number. Finite difference methods are developed for solving the space boundary value problems simultaneously, which are associated with these three equations. The applicability of the inverse formulation and the numerical solution is demonstrated by obtaining a solution to the three-dimensional, free surface flow past a vertical strut which extends through the fluid surface and is placed between channel walls.

Ia

DD FORM 1 NOV 65 1473 (PAGE 1)

S/N 0101-807-6801

unclassified

Security Classification

unclassified
Security Classification

| 14. KEY WORDS | LINK A | | LINK B | | LINK C | |
|---|---|---|---|---|---|---|
| | ROLE | WT | ROLE | WT | ROLE | WT |
| Inviscid flow | | | | | | |
| Three-Dimensional | | | | | | |
| Finite differences | | | | | | |
| Inverse Formulation | | | | | | |
| Free surface gravity | | | | | | |

Ib

DD FORM 1 NOV 65 1473 (B

(PAGE 2)

Unclassified
Security Classification

# STUDIES TO DEVELOP AND INVESTIGATE AN INVERSE FORMULATION FOR NUMERICALLY SOLVING THREE-DIMENSIONAL FREE SURFACE POTENTIAL FLUID FLOWS

by

Roland W. Jeppson

This research was carried out under the
Naval Ship Systems Command
General Hydromechanics Research Program
Subproject SR 009 01 01 administered by the
Naval Ship Research and Development Center
Contract No. N00014-67-A-0[illegible]20-0003





Utah Water Research Laboratory
College of Engineering
Utah State University
Logan, Utah 84321

IC

March 1972 PRWG-96-1

## ABSTRACT

An inverse formulation is developed for solving three-dimensional potential fluid flows which considers the magnitudes of the cartesian coordinates x, y, and z as the dependent variables in the space defined by the potential function and two mutually orthogonal stream surface functions whose intersection defines the physical space streamlines. This formulation reverses the usual role of the variables. In this inverse space irregular boundaries, with unknown position in the physical space, such as free surfaces become plane boundaries, and the space of most potential flow problems is a parallelepiped.

The basic partial differential equations resulting from this formulation are nonlinear and three in number. Finite difference methods are developed for solving the space boundary value problems simultaneously, which are associated with these three equations. The applicability of the inverse formulation and the numerical solution is demonstrated by obtaining a solution to the three-dimensional, free surface flow past a vertical strut which extends through the fluid surface and is placed between channel walls.

**Preceding page blank**

## TABLE OF CONTENTS

## LIST OF FIGURES



## LIST OF TABLES

# NOTATION

$\vec{A}$ = any vector quantity

$a$ = $\partial x/\partial \phi$

$a_g$ = acceleration of gravity

$\vec{B}$ = any vector quantity

$b$ = $\partial y/\partial \phi$

$c$ = $\partial z/\partial \phi$

$c_1$ = $D/M_1$

$D$ = depth of upstream flow

$D$ = derivative determinant

$d$ = $\partial y/\partial \psi$

$e$ = $\partial z/\partial \psi^*$

$F$ = denotes function of

$f$ = denotes function of

$f$ = $\partial y/\partial \psi^*$

$\vec{f}$ = vector array of values

$G$ = denotes function of

$g$ = denotes function of

$g$ = $\partial z/\partial \psi$

$H$ = depth of flow plus velocity head

$H$ = denotes function of

$h$ = denotes function of

$h$ = $\partial x/\partial \psi^*$

$i$ = subscript denoting increment in $\phi$ direction

$\vec{i}$ = unit vector in x-direction

$J$ = Jacobian determinant

$j$ = inverse Jacobian determinant

$j$ = subscript denoting increment in $\psi$ direction

$\vec{j}$ = unit vector in y-direction

$k$ = subscript denoting increment in $\psi^*$ direction

$\vec{k}$ = unit vector in z-direction

$L$ = number of $\phi$ grid planes

$L_1$ = $L - 1$

$M$ = number of $\psi$ grid planes

$M_1$ = $M - 1$

$N$ = number of $\psi^*$ grid planes

$N_1$ = $N - 1$

$NS$ = $\psi^*$ plane coincident with strut

$p$ = superscript denoting iteration number

$Q$ = flow rate

$q$ = superscript denoting iteration number

$\vec{q}$ = vector array of values

$\vec{r}$ = vector array of values

$\vec{s}$ = vector array of values

$u$ = velocity component in x-direction

$v$ = velocity component in y-direction

$w$ = velocity component in z-direction

$w_1$ = over-relaxation factor

| | | |
|---|---|---|
| $W$ | = | width of channel |
| $x$ | = | cartesian coordinate and also magnitude thereof |
| $y$ | = | cartesian coordinate and also magnitude thereof |
| $z$ | = | cartesian coordinate and also magnitude thereof |
| $\alpha$ | = | direction cosine |
| $\beta$ | = | direction cosine |
| $\vec{\nabla}$ | = | $\vec{i}\frac{\partial}{\partial x} + \vec{j}\frac{\partial}{\partial y} + \vec{k}\frac{\partial}{\partial z}$ |
| $\gamma$ | = | direction cosine |
| $\theta$ | = | angle |
| $\pi$ | = | 3.1417 |
| $\Phi$ | = | potential function |
| $\phi$ | = | dimensionless potential function |
| $\Psi$ | = | stream surface function |
| $\dot{\psi}$ | = | dimensionless stream surface function |
| $\Psi^*$ | = | stream surface function |
| $\psi^*$ | = | dimensionless stream surface function |

# INTRODUCTION

For many practical fluid flow problems in which viscous forces are of minor importance, because they are confined to relatively small regions of the flow, inviscid fluid flow theory yields results which are adequate for most applications. Consequently a vast amount of literature deals with inviscid fluid flow theory. Despite all of the effort represented by this literature, many relatively common problems with free surfaces and/or cavities have not been solved in closed form without introducing a number of simplifying assumptions which are not in accord with real situations. Available analytic methods generally require that the fluid be assumed weightless (i.e. the acceleration of gravity is zero). Furthermore, since such methods are based on complex variables, they are restricted to plane two-dimensional flows. Consequently, in order to solve problems with free surfaces under the influence of gravity, or three-dimensional problems even if axially symmetric, researchers have been forced to obtain solutions based on numerical approximations rather than solving the problems in closed form.

The application of finite differences constitutes one of the most powerful and universally applicable methods for obtaining such approximate solutions. The use of finite differences for solving free streamline problems in the physical plane is extremely difficult since the position of the free streamlines is unknown *a priori*. The solution can be obtained only through a process of repeatedly adjusting the assumed position of the free streamlines, through considerable insight and judgment, until all conditions of the problem are satisfied. Since the means for determining whether all conditions are satisfied is often quite insensitive to the position of the free streamlines, it is difficult to determine the reliability of the resulting approximate solution, and consequently the literature contains a number of examples where subsequent analyses have demonstrated that considerable error resulted because of an incorrect position of the free streamline.

An approach for solving two-dimensional fluid flow problems which is superior in many regards to a formulation in the physical plane, particularly if free surfaces are present, is to interchange the usual role of variables in the problem. Such inverse formulations have used the potential function, $\phi$, and the stream function, $\psi$, as the independent variables, and as dependent variables such quantities as: (1) the magnitude of the cartesian coordinates x and y, (2) the angle of the direction of flow, $\theta$, and the logarithm of the magnitude of the velocity, log $|V|$, or (3) the magnitudes of the horizontal and vertical components of the velocity, u and v. A major advantage to such an inverse formulation is that free surfaces, being streamlines along which $\psi$ is constant, become straight boundaries in the $\phi\psi$ plane, and many problems are consequently confined within rectangular regions. Also the results from a solution are in an ideal form for plotting a flownet and are well adapted for computing other quantities of interest concerning the flow.

This type of inverse formulation, accompanied by a subsequent finite difference solution, has been used to study a variety of two-dimensional free streamline problems (Thom and Apelt, 1961; Cassidy, 1965; Markland, 1965; Jeppson, 1966 and 1969a). The same approach has been used to solve problems dealing with plane saturated porous media flow with phreatic or free surfaces (Jeppson, 1968a, b, and c), and unsaturated moisture movement in soils (Jeppson and Nelson, 1970, and Jeppson et al., 1972). The same approach of using a formulation which interchanges the usual role of the variables with an accompanying numerical solution has been used to solve three-dimensional problems with axial symmetry. In these problems the magnitude of the radial and axial coordinates r and z are made dependent in the plane of the potential function and Stokes' stream function (or logarithm thereof). (See Jeppson, 1966; Mackenroth and Fisher, 1968; Jeppson, 1968d, 1969b and 1970.)

The work reported herein extends the inverse formulation technique which has been used in solving plane and axisymmetric potential fluid flow problems to general three-dimensional potential fluid flow problems and demonstrates the applicability of the methods by obtaining a numerical solution to the three-dimensional flow in an open channel past a strut. While this problem is a very simple three-dimensional problem for which a two-dimensional analysis (or for some features a one-dimensional analysis) may be adequate, it does include the common boundary conditions found in most problems. Furthermore, because of the simplicity of the problem, the adequacy or inadequacies of the numerical solution can more readily be ascertained and where necessary, modifications made. Consequently the results from the problem solution have the primary purpose of illustrating the method of inversely formulating and solving a three-dimensional free surface flow problem. With a better understanding of the performance of various numerical schemes in solving inversely formulated three-dimensional problems, the next step would be to apply the methods to more complex three dimensional flows.

# INVERSE FORMULATION

## Selection of variables

The first step in developing an inverse formulation to three-dimensional potential flows is the selection of three appropriate dependent and three appropriate independent variables. Since the best inverse approaches in the literature to plane and axisymmetric flow problems have considered the magnitudes of the coordinates x and y or r and z as dependent variables, the magnitudes of the cartesian coordinates x, y, and z should constitute appropriate dependent variables in an inverse formulation to a three-dimensional problem. This same literature suggests that the potential function as well as some functions to define the flow paths would constitute appropriate independent variables, or define the space within which the problem is defined. The functions selected for defining the flow paths consist of two stream surfaces which are tangent to the velocity vector. Yih (1957) has given equations for defining two such stream functions which will be denoted by $\psi$ and $\psi^*$ in this report. Nelson (1963) has given equivalent definitions for use in three-dimensional porous media flow applications.

The basic equations in these definitions are:

$$u = \Psi_y \Psi_z^* - \Psi_z \Psi_y^* = \Phi_x \quad \ldots . (1)$$

$$v = \Psi_z \Psi_x^* - \Psi_x \Psi_z^* = \Phi_y \quad \ldots . (2)$$

$$w = \Psi_x \Psi_y^* - \Psi_y \Psi_x^* = \Phi_z \quad \ldots . (3)$$

in which u, v, and w are the components of the velocity vector V in the x, y, and z coordinate directions respectively, i.e. $\vec{V} = u\vec{i} + v\vec{j} + w\vec{k}$, and the subscripts denote partial derivatives in the usual manner, i.e. $\Psi_z = \partial\Psi / \partial z$, etc. It can easily be shown that Eqs. 1, 2, and 3 reduce to the well known equations $\Psi_y = \Phi_x$ and $\Psi_x = -\Phi_y$ for the special case of plane potential flows. In vector notation Eqs. 1, 2, and 3 become

$$\vec{V} = (\text{grad}\,\Psi) \times (\text{grad}\,\Psi^*) = \text{grad}\,\Phi \quad \ldots (4)$$

## Transformation from physical space to $\Phi\Psi\Psi^*$ space

To obtain the basic inverse equations note that since the potential function and the two stream functions are functions of x, v, and z, i.e. $\Phi = F(x,y,z)$, $\Psi = G(x,y,z)$ and $\Psi^* = H(x,y,z)$, it follows that x, y, and z must also be functions of $\Phi$, $\Psi$, and $\Psi^*$, i.e. $x = f(\Phi, \Psi, \Psi^*)$, $y = g(\Phi, \Psi, \Psi^*)$, and $z = h(\Phi, \Psi, \Psi^*)$. Using the chain rule to differentiate $x = f(\Phi, \Psi, \Psi^*)$ with respect to x, y, and z respectively gives

$$\begin{aligned} 1 &= x_\Phi F_x + x_\Psi G_x + x_{\Psi^*} H_x \\ 0 &= x_\Phi F_y + x_\Psi G_y + x_{\Psi^*} H_y \\ 0 &= x_\Phi F_z + x_\Psi G_z + x_{\Psi^*} H_z \end{aligned} \quad \ldots\ldots (5)$$

Solving these three equations for the unknowns $x_\Phi$, $x_\Psi$, and $x_{\Psi^*}$ gives

$$x_\Phi = \frac{1}{J}\frac{\partial(G,H)}{\partial(y,z)}, \quad x_\Psi = -\frac{1}{J}\frac{\partial(F,H)}{\partial(y,z)},$$

$$\text{and } x_{\Psi^*} = \frac{1}{J}\frac{\partial(F,G)}{\partial(y,z)} \quad \ldots\ldots . (6)$$

in which J is the Jacobian given by the determinant

$$J = \begin{vmatrix} F_x & F_y & F_z \\ G_x & G_y & G_z \\ H_x & H_y & H_z \end{vmatrix}$$

and the derivatives of the quantities enclosed in parentheses denote minor determinants in the usual way, i.e.

$$\frac{\partial(G,H)}{\partial(y,z)} = G_y H_z - G_z H_y$$

Differentiating $y = g(\Phi, \Psi, \Psi^*)$ with respect to x, y, and z respectively and solving the three equations gives

$$y_\Phi = -\frac{1}{J}\frac{\partial(G,H)}{\partial(x,z)}, \quad y_\Psi = \frac{1}{J}\frac{\partial(F,H)}{\partial(x,z)},$$

$$y_{\Psi^*} = -\frac{1}{J}\frac{\partial(F,G)}{\partial(x,z)} \quad \ldots\ldots \; (7)$$

Likewise differentiation of $z = h(\Phi, \Psi, \Psi^*)$ leads to,

$$z_\Phi = \frac{1}{J}\frac{\partial(G,H)}{\partial(x,y)}, \quad z_\Psi = -\frac{1}{J}\frac{\partial(F,H)}{\partial(x,y)},$$

$$z_{\Psi^*} = \frac{1}{J}\frac{\partial(F,G)}{\partial(x,y)} \quad \ldots\ldots\ldots \; (8)$$

Following the same procedure as that above but solving for $\Phi_x$, $\Phi_y$, ..., $\Psi_x$, ..., $\Psi^*_z$ gives

$$\Phi_x = \frac{1}{j}\frac{\partial(y,z)}{\partial(\Psi,\Psi^*)}, \quad \Phi_y = -\frac{1}{j}\frac{\partial(x,z)}{\partial(\Psi,\Psi^*)}, \quad \Phi_z = \frac{1}{j}\frac{\partial(x,y)}{\partial(\Psi,\Psi^*)}$$

$$\Psi_x = -\frac{1}{j}\frac{\partial(y,z)}{\partial(\Phi,\Psi^*)}, \quad \Psi_y = \frac{1}{j}\frac{\partial(x,z)}{\partial(\Phi,\Psi^*)}, \quad \Psi_z = -\frac{1}{j}\frac{\partial(x,y)}{\partial(\Phi,\Psi^*)}$$

$$\Psi^*_x = \frac{1}{j}\frac{\partial(y,z)}{\partial(\Phi,\Psi)}, \quad \Psi^*_y = -\frac{1}{j}\frac{\partial(x,z)}{\partial(\Phi,\Psi)}, \quad \Psi^*_z = \frac{1}{j}\frac{\partial(x,y)}{\partial(\Phi,\Psi)}. \quad (9)$$

in which j is the inverse Jacobian determinant

$$j = \begin{vmatrix} f_\Phi & f_\Psi & f_{\Psi^*} \\ g_\Phi & g_\Psi & g_{\Psi^*} \\ h_\Phi & h_\Psi & h_{\Psi^*} \end{vmatrix} = \frac{1}{J}$$

By substituting from Eqs. 6, 7, 8, and 9 into Eqs. 1, 2, and 3, the following three inverse equations are obtained:

$$x_\Phi = y_\Psi z_{\Psi^*} - y_{\Psi^*} z_\Psi \quad \ldots\ldots \; (10)$$

$$y_\Phi = x_{\Psi^*} z_\Psi - x_\Psi z_{\Psi^*} \quad \ldots\ldots \; (11)$$

$$z_\Phi = x_\Psi y_{\Psi^*} - x_{\Psi^*} y_\Psi \quad \ldots\ldots \; (12)$$

These three equations are the basic inverse equations which define the dependent variables x, y, and z in the $\Phi\Psi\Psi^*$ space, just as Eqs. 1, 2, and 3 are the basic equations for $\Phi$, $\Psi$, and $\Psi^*$ in the physical space. Consequently, when associated with appropriate boundary conditions for a particular problem, the simultaneous solution of Eqs. 10, 11, and 12 would constitute the solution to that particular problem. Before discussing methods for solving these equations some properties of the stream surfaces $\Psi$ and $\Psi^*$ will be presented.

**Properties of stream surfaces**

The definitions for stream functions $\Psi$ and $\Psi^*$ as given by Eqs. 1, 2, and 3 (or Eq. 4) satisfy the incompressible, steady state continuity equation $\nabla \cdot \vec{V} \equiv 0$. This can be verified from the vector identity $\nabla \cdot (\vec{A} \times \vec{B}) = \vec{B} \cdot (\nabla \times \vec{A}) - \vec{A} \cdot (\nabla \times \vec{B})$. Thus from Eq. 4,

$$\nabla \cdot \vec{V} = \nabla\Psi^* \cdot (\nabla \times \nabla\Psi) - \nabla\Psi \cdot (\nabla \times \nabla\Psi^*) \quad \ldots\ldots (13)$$

but the curl of the gradient of any scalar function is zero and therefore $\nabla \times \nabla\Psi \equiv 0$ and $\nabla \times \nabla\Psi^* \equiv 0$, with the result that

$$\nabla \cdot \vec{V} = \nabla \cdot (\nabla\Psi \times \nabla\Psi^*) \equiv 0 \quad \ldots\ldots\ldots (14)$$

The stream surfaces defined by holding both $\Psi$ and $\Psi^*$ constant are orthogonal to the equipotential surfaces defined by holding $\Phi$ constant. Orthogonality exists provided the dot products of the gradients are identically equal to zero. Using Eqs. 1, 2, and 3 it can readily be shown that $\nabla\Phi \cdot \nabla\Psi \equiv 0$ and $\nabla\Phi \cdot \nabla\Psi^* \equiv 0$ and therefore the equipotential surfaces are everywhere at right angles to the surfaces defined by holding the two stream functions constant.

In general, the definitions for $\Psi$ and $\Psi^*$ do not require that the surfaces defined by holding $\Psi$ and $\Psi^*$ constant are orthogonal to each other. However, in the previously given inverse equations it is necessary that of the many $\Psi$ and $\Psi^*$ equal constant surfaces which exist, only those are selected which constitute an orthogonal pair so that the inverse coordinates $\Phi$, $\Psi$, and $\Psi^*$ are independent. The use of the inverse formulation assumes that using $\Phi$, $\Psi$, and $\Psi^*$ as orthogonal coordinates insures that appropriate orthogonal $\Psi$ and $\Psi^*$ stream surfaces are selected. Perhaps a more fundamental approach would impose the condition $\nabla\Psi \cdot \nabla\Psi^* \equiv 0$ directly. Methods for imposing this condition directly are not apparent, however.

# METHODS FOR SOLVING INVERSF EQUATIONS

**Alternatives available**

Considerable guidance in the selection of the independent and dependent variables for the three-dimensional problem was provided by past inverse solutions to plane flow problems. Less guidance is available from these past solutions regarding the best methods for solving the three-dimensional inverse equations. Since the basic equations (Eqs. 10, 11, and 12) are nonlinear, and each equation contains all three dependent variables x, y, and z, it is clear that numerical methods offer the best presently available approach to a solution. In solving the comparable equations,

$$x_\Phi = y_\Psi \quad \ldots\ldots\ldots (15)$$

$$x_\Psi = - y_\Phi \quad \ldots\ldots\ldots (16)$$

from plane potential flows, the equations are first combined by differentiation to obtain equations involving only one dependent variable. These equations for plane flows are the inverse Laplacian equations $\nabla^2_{\phi\psi} x = 0$ and $\nabla^2_{\phi\psi}\ y = 0$. Because of the products present in the terms on the right side of the equal sign in Eqs. 10, 11, and 12, reasonably simple equations with only one dependent variable cannot be obtained by differentiation and combination as can be done for the equivalent plane flow equations. Consequently an alternative approach for solving the inverse three-dimensional equations must be sought.

An alternate which may appear feasible at first would utilize finite difference methods to obtain a simultaneous solution to the boundary value problems associated with the three first order partial differential Equations 10, 11, and 12. An examination of the finite difference equations obtained from these three equations by approximating the derivatives with second or higher order differences indicates that point by point iterative methods, such as Gauss-Seidel or SOR method would not be convergent. Such iterative methods would diverge simply because the coefficient associated with the value of the variable at the grid point in question is less in magnitude than the sum of the coefficients of the other terms. In a linear system the equivalent would be a nondiagonally dominant coefficient matrix. But since diagonal dominance is a necessary condition for point by point methods to converge, it may be concluded that only if first order forward or backward differences are used to replace the derivative in Eqs. 10, 11, and 12 would it be possible to solve the boundary value problems associated with the first order equations simultaneously. Because of the low order approximation of first order differences this possibility for solution was not considered initially. (Using a weighting all possible first differences which depend upon the distance from the boundary, a workable method results. This approach is under investigation in the same project.) Rather three alternatives were investigated.

The first alternative is to use block iterative methods to solve the finite difference equations obtained from third order difference approximations of the derivatives in the first order partial differential equations. The merits of this approach were actually investigated by implementing its use in computer programs which solved the finite difference equations across an entire line of grid points, and across two adjacent lines simultaneously for the two-dimensional problems of corner flow. The conclusion was that these block (i.e. line) iterative methods were also nonconvergent. Later study has, however, shown that what was considered nonconvergence may have actually been due to the poor approximation of the finite difference solution to the actual corner flow. Regardless of the incorrectness of the above conclusion, the use of block iterative methods for solving the simultaneous boundary value problems was not pursued further. Rather the method of approach which is described in this report was developed and implemented in a computer program for solving three-dimensional flow around a strut.

The third alternative which has been studied for solving the simultaneous boundary value problems will be described more fully in a subsequent report containing the results of a Ph.D. thesis by Allen Davis. Basically this later alternative also uses Eqs. 10, 11, and 12 in their present forms, and obtains a simultaneous solution for x, y, and z from the difference equations obtained by third order approximations at all grid points on an entire plane within the flow space. The resulting finite difference equations become linear under the assumption that values on adjacent planes are known. Consequently the solution on each plane can be obtained efficiently by utilizing techniques for grouping the nonzero elements of the coefficient matrix into bands, and implementing

algorithms which take advantage of the zero elements of the matrix. By repeatedly obtaining such solutions, plane by plane and subsequently repeating the entire process until the absolute sum of changes in all three variables at all grid points became less than some error parameter, the final solution should result. In essence this alternative is an extension of block iterative methods to a space boundary value problem in which the block becomes an entire plane and direct methods are used to solve the finite difference equations in that plane. For some yet unknown reason this procedure neither converges to, nor diverges from, the final solution. A more detailed description of the implementation of this method and its inadequacy will be given in a subsequent report.

The method of solution described in this report does not use Eqs. 10, 11, and 12 directly in their present form. Rather these three equations are combined by differentiation, under the assumption that certain of the derivatives are known, in such a way that quasi-separate equations are developed for each variable x, y, and z in different planes within the $\phi\psi\psi^*$ space. The magnitude of the assumed known quantities in these separate equations can only be determined approximately until the final solution is obtained. Consequently these assumed known quantities are repeatedly adjusted in a cycle of solutions until their correct values are obtained.

**Nondimensionalizing independent variables**

Before demonstrating how such quasi-separate equations can be obtained, Eqs. 10, 11, and 12 will be transformed so the new independent variables $\phi$, $\psi$, and $\psi^*$ are dimensionless as given by the following three equations

$$\phi = \frac{N_1 D \Phi}{Q} \quad \ldots\ldots\ldots (17)$$

$$\psi = \frac{M_1 \Psi}{\sqrt{Q}} \quad \ldots\ldots\ldots (18)$$

$$\psi^* = \frac{N_1 \Psi^*}{\sqrt{Q}} \quad \ldots\ldots\ldots (19)$$

in which D is the undisturbed depth of flow in the channel, Q is the total volumetric flow rate in the channel, $N_1$ is the number of grid increments in the $\psi^*$ direction and $M_1$ is the number of grid increments in the $\psi$ direction. Transforming Eqs. 10, 11, and 12 by means of Eqs. 17, 18, and 19 leads to

$$c_1 \overset{a}{\acute{x}_\phi} = \overset{d}{\acute{y}_\psi} \overset{e}{\acute{z}_{\psi^*}} - \overset{f}{\acute{y}_{\psi^*}} \overset{g}{\acute{z}_\psi} \quad \ldots\ldots (20)$$

$$c_1 \overset{b}{\acute{y}_\phi} = \overset{h}{\acute{x}_{\psi^*}} \overset{g}{\acute{z}_\psi} - \overset{i}{\acute{x}_\psi} \overset{e}{\acute{z}_{\psi^*}} \quad \ldots\ldots (21)$$

$$c_1 \overset{c}{\acute{z}_\phi} = \overset{i}{\acute{x}_\psi} \overset{f}{\acute{y}_{\psi^*}} - \overset{h}{\acute{x}_{\psi^*}} \overset{d}{\acute{y}_\psi} \quad \ldots\ldots (22)$$

in which $c_1 = D/M_1$, and the single letter over the individual derivatives will be used subsequently whenever that derivative is assumed to be known.

**Development of quasi-separate equations for x, y, and z**

To demonstrate how separate quasi-separate equations for x, y, and z, which apply on an individual plane within the $\phi\psi\psi^*$ space, might be developed, Eqs. 20 and 21 are written below assuming that derivatives with respect to $\psi^*$ are known and that the variable z is known.

$$c_1 x_\phi = e y_\psi - fg \quad \ldots\ldots\ldots (20a)$$

$$c_1 y_\phi = hg - e x_\psi \quad \ldots\ldots\ldots (21a)$$

Upon differentiating Eq. 20a with respect to $\phi$ and Eq. 21a with respect to $\phi$ and eliminating $y_{\phi\psi} = y_{\psi\phi}$ gives

$$c_1 x_{\phi\phi} + \frac{e}{c_1}\left[e x_{\psi\psi} + x_\psi e_\psi - (gh)_\psi\right] - \frac{e_\phi}{e}(c_1 x_\phi + fg) + (fg)_\phi = 0 \quad \ldots\ldots\ldots\ldots (23)$$

Likewise differentiating Eq. 20a with respect to $\psi$ and Eq. 21a with respect to $\phi$ and combining the resulting equations gives the following equation for y in $\phi\psi$ planes,

$$c_1 y_{\phi\phi} + \frac{e}{c_1}\left[e y_{\psi\psi} + y_\psi e_\psi - (fg)_\psi\right] + \frac{e_\phi}{e}(gh - c_1 y_\phi) - (gh)_\phi = 0 \quad \ldots\ldots\ldots\ldots (24)$$

If y had been considered known along with derivatives with respect to $\psi^*$ in Eqs. 20 and 22 the same procedure as that given above would have resulted in equations for x and z in the $\phi\psi$ planes. Equations for y and z would result if x were considered known. In fact for each pair of equations which can be formed from Eqs. 20, 21, and 22, two quasi-separate equations would result under each assumption of known variables. Table 1 lists the 18 equations that can be obtained in this manner, and indicates in which plane each of these equations applies as well as from which two of the three basic equations it was obtained.

The motivation for combining Eqs. 20, 21, and 22 by differentiation into the second order partial differential equations in Table 1 is to obtain second derivatives in the equation, for which second order central difference approximations lead to diagonally dominant coefficient matrices. The equations in Table 1 also have some resemblance to Laplacian type equations for which the common finite difference methods have been developed. Perhaps the greatest motivation for developing the equations in Table 1, however, was to have separate equations from which to solve each of the dependent variables x, y, and z.

**Criteria for selecting best suited equations**

Generally in solving any particular problem, only one equation for each of the unknowns x, y, and z would be used. Should considerable differences exist in the flow patterns in different regions of a particular problem it may be desirable to use different equations in different regions. The success and efficiency of obtaining a solution by use of the equations in Table 1 depends upon the selection of the equation which will be used to solve for each of the unknowns. While there are additional criteria which might help in making this selection it appears that the following three items are important: (1) The assumptions of known derivatives should be made as valid as possible; that is the values, denoted by single letters in the equation that is used, should be maintained as constant as possible during the solution process which would start with an initialization and proceed until all conditions of the problem are satisfied. (2) That the coefficients of the two second derivative terms in the equation be as nearly equal as possible. For the last three equations in Table 1, obviously at least one of the single lettered values must be negative so that the PDE is elliptic. (3) That the magnitudes of the terms involving first derivatives be maintained as small as possible.

Several reasons exist for citing these criteria. First if the single lettered values, which are assumed to be known during the process of obtaining a solution on any plane, have their values altered greatly between successive solutions in that plane, they will obviously affect the results from these consecutive solutions. These solution results, in turn, could affect the magnitudes of the coefficients. If, however, the lettered coefficients are nearly correct at initialization, or if their magnitudes have a minor influence on the solution, the final solution will be obtained in fewer total arithmetic operations.

The basis for the second criteria is to make the solution in each of the planes of the space equally dependent upon all four of its boundary values (or boundary conditions), and not more dependent on two opposite boundaries than on the other two opposite boundaries. This latter condition would occur if the coefficient of one of the second derivatives was very small in comparison to the other. The second criteria also helps insure that the equation has some resemblance to Laplaces equation for which many numerical, as well as other, solutions have been obtained. Should this criteria be strongly violated, a solution in each individual plane may be obtained with fewer numerical calculations by simultaneously solving the system of finite difference equations along the grid lines in the direction of the independent variable whose derivative has the larger coefficient. Since the problem is of the elliptic type, this would mean that a high dependency must exist between the values on this plane and those on adjacent planes. Consequently, any reduction in arithmetic calculations in obtaining individual solutions would be more than offset by more cycles of such solutions. Furthermore, the solution process may be less likely to be convergent. Consequently satisfying the second criteria simultaneously helps assume that the first criteria is satisfied.

An illustration of how these criteria aid in the selection of the equation which will be used to solve each of the dependent variables x, y, and z is given later in the discussion of the problem of flow around a strut in a channel.

To obtain a better understanding of how rapidly, or whether, iterative finite difference methods would converge for the equations in Table 1, individual computer programs were written to solve each of the equations in Table 1. For each such problem Dirichlet boundary conditions were specified, and algorithms implementing both the successive over-relaxation (SOR) method and the line successive over-relaxation (LSOR) method (see Forsythe and Wasow, 1960, or Varga, 1962) were tested. In part the criteria given for selecting the best equations for solving a particular problem were arrived at from noting and comparing the performance of these separate programs in obtaining a solution. The performance of those programs implementing solutions to Eqs. 35 through 40 in $\psi\psi^*$ planes was generally considerably poorer than those implementing solutions in either $\phi\psi$ or $\phi\psi^*$ planes. If a poor initialization of all unknowns was used when solving the equations in $\psi\psi^*$ planes, solutions did not result, but rather rapid divergence occurred. When such lack of convergence occurred it appeared to be associated with initializations which at some grid points caused the coefficients of the second derivative terms to have opposite signs, or which caused the magnitudes of

**Table 1. Quasi-separate equations obtained from Eqs. 20, 21, and 22 by assuming some variables were known.**

| Eq. No. | Derived from Eqs. | Plane of Equation | Quasi-Separate Partial Diff. Eq. |
|---|---|---|---|
| 23 | 20 & 21 | $\phi\psi$ | $c_1x_{\phi\phi} + \frac{e}{c_1}[ex_{\psi\psi} + e_\psi x_\psi - (gh)_\psi] - \frac{e_\phi}{e}(c_1x_\phi + fg) + (fg)_\phi = 0$ |
| 24 | 20 & 21 | $\phi\psi$ | $c_1y_{\phi\phi} + \frac{e}{c_1}[ey_{\psi\psi} + e_\psi y_\psi - (fg)_\psi] + \frac{e_\phi}{e}(gh - c_1y_\phi) - (gh)_\phi = 0$ |
| 25 | 20 & 22 | $\phi\psi$ | $c_1x_{\phi\phi} + \frac{f}{c_1}[fx_{\psi\psi} + f_\psi x_\psi - (dh)_\psi] + \frac{f_\phi}{f}(de - c_1x_\phi) - (de)_\phi = 0$ |
| 26 | 20 & 22 | $\phi\psi$ | $c_1z_{\phi\phi} + \frac{f}{c_1}[fz_{\psi\psi} + f_\psi z_\psi - (de)_\psi] - \frac{f_\phi}{f}(c_1z_\phi + dh) + (dh)_\phi = 0$ |
| 27 | 21 & 22 | $\phi\psi$ | $c_1y_{\phi\phi} + \frac{h}{c_1}[hy_{\psi\psi} + h_\psi y_\psi - (if)_\psi] - \frac{h_\phi}{h}(c_1y_\phi + ie) + (ie)_\phi = 0$ |
| 28 | 21 & 22 | $\phi\psi$ | $c_1z_{\phi\phi} + \frac{h}{c_1}[hz_{\psi\psi} + h_\psi z_\psi - (ie)_\psi] + \frac{h_\phi}{h}(if - c_1z_\phi) - (if)_\phi = 0$ |
| 29 | 20 & 21 | $\phi\psi^*$ | $c_1x_{\phi\phi} + \frac{g}{c_1}[gx_{\psi^*\psi^*} + g_{\psi^*}x_{\psi^*} - (ie)_{\psi^*}] + \frac{g_\phi}{g}(de - c_1x_\phi) - (de)_\phi = 0$ |
| 30 | 20 & 21 | $\phi\psi^*$ | $c_1y_{\phi\phi} + \frac{g}{c_1}[gy_{\psi^*\psi^*} + g_{\psi^*}y_{\psi^*} - (de)_{\psi^*}] - \frac{g_\phi}{g}(c_1y_\phi + ie) + (ie)_\phi = 0$ |
| 31 | 20 & 22 | $\phi\psi^*$ | $c_1x_{\phi\phi} + \frac{d}{c_1}[dx_{\psi^*\psi^*} + d_{\psi^*}x_{\psi^*} - (if)_{\psi^*}] + \frac{d_\phi}{d}(c_1x_\phi + fg) + (fg)_\phi = 0$ |
| 32 | 20 & 22 | $\phi\psi^*$ | $c_1z_{\phi\phi} + \frac{d}{c_1}[dz_{\psi^*\psi^*} + d_{\psi^*}z_{\psi^*} - (fg)_{\psi^*}] + \frac{d_\phi}{d}(if - c_1z_\phi) + (if)_\phi = 0$ |
| 33 | 21 & 22 | $\phi\psi^*$ | $c_1y_{\phi\phi} + \frac{i}{c_1}[iy_{\psi^*\psi^*} + i_{\psi^*}y_{\psi^*} - (dh)_{\psi^*}] + \frac{i_\phi}{i}(gh - c_1y_\phi) - (gh)_\phi = 0$ |
| 34 | 21 & 22 | $\phi\psi^*$ | $c_1z_{\phi\phi} + \frac{i}{c_1}[iz_{\psi^*\psi^*} + i_{\psi^*}z_{\psi^*} - (gh)_{\psi^*}] - \frac{i_\phi}{i}(c_1z_\phi + dh) + (dh)_\phi = 0$ |
| 35 | 20 & 21 | $\psi\psi^*$ | $fhz_{\psi\psi} - diz_{\psi^*\psi^*} + (dh_{\psi^*} + hf_\psi)z_\psi - (di_{\psi^*} + hd_\psi)z_{\psi^*} - c_1(db_{\psi^*} + ha_\psi) = 0$ |
| 36 | 20 & 21 | $\psi\psi^*$ | $fhz_{\psi\psi} - diz_{\psi^*\psi^*} + (fh_\psi + if_{\psi^*})z_\psi - (id_{\psi^*} + fi_\psi)z_{\psi^*} + c_1(ia_{\psi^*} - fb_\psi) = 0$ |
| 37 | 20 & 22 | $\psi\psi^*$ | $ehy_{\psi\psi} - giy_{\psi^*\psi^*} + (he_\psi + gh_{\psi^*})y_\psi - (gi_{\psi^*} + hg_\psi)y_{\psi^*} + c_1(gc_{\psi^*} - ha_\psi) = 0$ |
| 38 | 20 & 22 | $\psi\psi^*$ | $ehy_{\psi\psi} - giy_{\psi^*\psi^*} + (ie_{\psi^*} + eh_\psi)y_\psi - (ig_{\psi^*} + ei_\psi)y_{\psi^*} + c_1(ec_\psi - ia_{\psi^*}) = 0$ |
| 39 | 21 & 22 | $\psi\psi^*$ | $efx_{\psi\psi} - dgx_{\psi^*\psi^*} + (gf_{\psi^*} + fe_\psi)x_\psi - (gd_{\psi^*} + fg_\psi)x_{\psi^*} + c_1(fb_\psi - gc_{\psi^*}) = 0$ |
| 40 | 21 & 22 | $\psi\psi^*$ | $efx_{\psi\psi} - dgx_{\psi^*\psi^*} + (de_{\psi^*} + ef_\psi)x_\psi - (dg_{\psi^*} + ed_\psi)x_{\psi^*} + c_1(db_{\psi^*} + ec_\psi) = 0$ |

these coefficients to take on small values. From this experience, the additional criteria may be added to the above three to avoid in general, one of the equations which apply on $\psi\psi^*$ planes.

The performance of the two algorithms (SOR and LSOR methods) which were implemented in the programs mentioned above indicated that generally less computer execution time was required by the LSOR method than the SOR method. No experimentation was done to examine the effect of the over-relaxation factor. All solutions under both methods used an over-relaxation factor equal to 1.4. Since the comparison was close, showing that the LSOR method required in the neighborhood of 20 to 40 percent less execution time than the SOR method, changes in over-relaxation factors might favor the SOR method. Furthermore, the outcome of such a comparison is computer system dependent, as well as being influenced by the particular statements in the source language written for each method. In the LSOR method more computations are involved per iteration but fewer iterations are required for a solution than with the SOR method. Since the additional computations per iteration are primarily with nonsubscripted variables or single arrayed variables, the LSOR method requires fewer operations with triple subscripted arrays. These comparisons were made on the UNIVAC 1108 system, under EXEC 8, at the University of Utah.

**Finite differences**

The finite difference operators have been obtained by replacing the derivatives in the equations in Table 1 with second order central difference approximations. The finite difference space network has been selected such that $\Delta\psi^* = \Delta\psi = \Delta\phi = 1$. The grid spacing increments $\Delta\psi^*$, $\Delta\psi$, and $\Delta\phi$ can each be equated to unity because the number of grid increments, $M_1$ and $N_1$ in the $\psi$ and $\psi^*$ directions, respectively, are included in Eqs. 17, 18, and 19 for defining the dimensionless coordinates $\phi$, $\psi$, and $\psi^*$. The motivation for introducing $M_1$ and $N_1$ in Eqs. 17, 18, and 19 was to allow these increments to be unity and thus eliminate a number of multiplications which would result from nonunity $\Delta$'s in the finite difference operators.

The finite difference operators for interior space grid points are given in Table 2 for the first 12 equations in Table 1. To make for easy reference the equation numbers given for each finite difference operator in Table 2 is the same as that for the PDE from which it was derived in Table 1. The forms of these finite difference operators, as given in Table 2, conform to that needed to apply the LSOR method along those lines defined by the incremented subscripts on the left side of the equal sign (i.e. in the direction of increasing $\phi$) and which lie in the plane on which the particular equation applies. The triple subscripts to x, y, and z in the finite difference operators are arranged in order so that the first corresponds to $\phi$, the second to $\psi$ and the third to $\psi^*$ as defined by

$$i = 1 + \phi/\Delta\phi \quad \ldots\ldots\ldots\ldots (41)$$

$$j = 1 + \psi/\Delta\psi \quad \ldots\ldots\ldots\ldots (42)$$

$$k = 1 + \psi^*/\Delta\psi^* \quad \ldots\ldots\ldots\ldots (43)$$

The $\alpha$'s in each finite difference operator are unique to that operator as defined in the right portion of the table. They are used to simplify the writing of the operators and consist of the combination, and/or derivatives, of the assumed temporarily known quantities given by a single letter in the PDE's in Table 1.

The operators in Table 2 can be rewritten readily to conform to that needed to apply them in the LSOR method in the other coordinate direction by interchanging the terms across the equal signs or for the SOR method by placing only the term with an ijk subscript on the left of the equal sign.

**Numerical operations involved in obtaining a solution**

As pointed out earlier, the solution or solutions on any given plane within the space of the problem must be obtained repeatedly; each subsequent solution hopefully will have more nearly correct coefficients which are assumed known, but which actually are dependent upon knowing the correct solutions to the other variables. Consequently, a single group of solutions on individual planes for x, y, and z will not be sufficient. Rather such groups of solutions must be obtained repeatedly until all coefficients are correct. To help describe the procedure used in obtaining the final complete finite difference solution to a three-dimensional problem, the following terminology will be used.

(a) *Tentative solution*–refers to a solution based on any of the finite difference operators in Table 2 (or any of the finite difference operators for a boundary condition as given later) on a specified plane within the $\phi\psi\psi^*$ space. These tentative solutions are based on the best values for the $\alpha$'s which can be computed at that stage in the solution process, and consequently they are only tentative, but the results of these solutions are needed to obtain better estimates of the $\alpha$'s in the operators for the other two dependent variables.

(b) *Iteration number*–refers to the number of times the LSOR-method (or whatever other method is being used) adjusts all the values of x, y, or z on the particular plane for which a given tentative solution is being obtained. A sufficient number of iterations are required for each tentative solution until the sum across all grid points of that plane of absolute changes in value of that dependent variable is less than the prescribed error parameter.

(c) *Cycle number* refers to the number of times all tentative solutions are obtained. Thus during the first

**Table 2. Finite difference operators which are based on the partial differential equations in Table 1.**

| Eq. No. | Finite Difference Operator | Definition of $\alpha$ Coefficients in Operator |
|---|---|---|
| 23 | $-(1+\alpha_3)x_{i-1jk} + 2(1+\alpha_1)x_{ijk} - (1-\alpha_3)x_{i+1jk}$<br>$= (\alpha_1-\alpha_2)x_{ij-1k} + (\alpha_1+\alpha_2)x_{ij+1k} + \alpha_4$ | $\alpha_1 = \frac{e^2}{c_1^2},\ \alpha_2 = \frac{ee_\psi}{2c_1^2},\ \alpha_3 = \frac{e_\phi}{2e},$<br>$\alpha_4 = \frac{(fg)_\phi}{c_1} - \frac{e}{c_1^2}(gh)_\psi - \frac{e_\phi(fg)}{c_1 e}$ |
| 24 | $-(1+\alpha_3)y_{i-1jk} + 2(1+\alpha_1)y_{ijk} - (1-\alpha_3)y_{i+1jk}$<br>$= (\alpha_1-\alpha_2)y_{ij-1k} + (\alpha_1+\alpha_2)y_{ij+1k} + \alpha_4$ | $\alpha_1 = \frac{e^2}{c_1^2},\ \alpha_2 = \frac{ee_\psi}{2c_1^2},\ \alpha_3 = \frac{e_\phi}{2e},$<br>$\alpha_4 = \frac{e_\phi(gh)}{c_1 e} - \frac{e}{c_1^2}(fg)_\psi - \frac{(gh)_\phi}{c_1}$ |
| 25 | $-(1+\alpha_3)x_{i-1jk} + 2(1+\alpha_1) - (1-\alpha_3)x_{i+1jk}$<br>$= (\alpha_1-\alpha_2)x_{ij-1k} + (\alpha_1+\alpha_2)x_{ij+1k} + \alpha_4$ | $\alpha_1 = \frac{f^2}{c_1^2},\ \alpha_2 = \frac{ff_\psi}{2c_1^2},\ \alpha_3 = \frac{f_\phi}{2f},$<br>$\alpha_4 = \frac{f_\phi(de)}{c_1 f} - \frac{f}{c_1^2}(dh)_\psi - \frac{(de)_\phi}{c_1}$ |
| 26 | $-(1+\alpha_3)z_{i-1jk} + 2(1+\alpha_1)z_{ijk} - (1-\alpha_3)z_{i+1jk}$<br>$= (\alpha_1-\alpha_2)z_{ij-1k} + (\alpha_1+\alpha_2)z_{ij+1k} + \alpha_4$ | $\alpha_1 = \frac{f^2}{c_1^2},\ \alpha_2 = \frac{ff_\psi}{2c_1^2},\ \alpha_3 = \frac{f_\phi}{2f},$<br>$\alpha_4 = \frac{(dh)_\phi}{c_1} - \frac{f}{c_1^2}(de)_\psi - \frac{f_\phi(dh)}{c_1 f}$ |
| 27 | $-(1+\alpha_3)y_{i-1jk} + 2(1+\alpha_1)y_{ijk} - (1-\alpha_3)y_{i+1jk}$<br>$= (\alpha_1-\alpha_2)y_{ij-1k} + (\alpha_1+\alpha_2)y_{ij+1k} + \alpha_4$ | $\alpha_1 = \frac{h^2}{c_1^2},\ \alpha_2 = \frac{hh_\psi}{2c_1^2},\ \alpha_3 = \frac{h_\phi}{2h},$<br>$\alpha_4 = \frac{(ie)_\phi}{c_1} - \frac{h}{c_1^2}(if)_\psi - \frac{h_\phi(ie)}{c_1 h}$ |
| 28 | $-(1+\alpha_3)z_{i-1jk} + 2(1+\alpha_1)z_{ijk} - (1-\alpha_3)z_{i+1jk}$<br>$= (\alpha_1-\alpha_2)z_{ij-1k} + (\alpha_1+\alpha_2)z_{ij+1k} + \alpha_4$ | $\alpha_1 = \frac{[illegible]^2}{c_1^2},\ \alpha_2 = \frac{hh_\psi}{2c_1^2},\ \alpha_3 = \frac{h_\phi}{2h},$<br>$\alpha_4 = \frac{h_\phi(if)}{c_1 h} - \frac{(if)_\phi}{c_1} - \frac{h}{c_1^2}(ie)_\psi$ |

Table 2. Continued.

| Eq. No. | Finite Difference Operator | Definition of α Coefficients in Operator |
|---|---|---|
| 29 | $-(1+\alpha_3)x_{i-1jk} + 2(1+\alpha_1)x_{ijk} - (1-\alpha_3)x_{i+1jk}$ <br> $= (\alpha_1-\alpha_2)x_{ijk-1} + (\alpha_1+\alpha_2)x_{ijk+1} + \alpha_4$ | $\alpha_1 = \frac{g^2}{c_1^2},\ \alpha_2 = \frac{gg_{\psi*}}{2c_1^2},\ \alpha_3 = \frac{g_\phi}{2g},$ <br> $\alpha_4 = \frac{g_\phi(de)}{c_1 g} - \frac{g}{c_1^2}(ie)_{\psi*} - \frac{(de)_\phi}{c_1}$ |
| 30 | $-(1+\alpha_3)y_{i-1jk} + 2(1+\alpha_1)y_{ijk} - (1-\alpha_3)y_{i+1jk}$ <br> $= (\alpha_1-\alpha_2)y_{ijk-1} + (\alpha_1+\alpha_2)y_{ijk+1} + \alpha_4$ | $\alpha_1 = \frac{g^2}{c_1^2},\ \alpha_2 = \frac{gg_{\psi*}}{2c_1^2},\ \alpha_3 = \frac{g_\phi}{2g},$ <br> $\alpha_4 = \frac{(ie)_\phi}{c_1} - \frac{g_\phi(ie)}{c_1 g} - \frac{g}{c_1^2}(de)_{\psi*}$ |
| 31 | $-(1+\alpha_3)x_{i-1jk} + 2(1+\alpha_1)x_{ijk} - (1-\alpha_3)x_{i+1jk}$ <br> $= (\alpha_1-\alpha_2)x_{ijk-1} + (\alpha_1+\alpha_2)x_{ijk+1} + \alpha_4$ | $\alpha_1 = \frac{d^2}{c_1^2},\ \alpha_2 = \frac{dd_{\psi*}}{2c_1^2},\ \alpha_3 = \frac{d_\phi}{2d},$ <br> $\alpha_4 = \frac{(fg)_\phi}{c_1} - \frac{d_\phi(fg)}{c_1 d} - \frac{d}{c_1^2}(if)_{\psi*}$ |
| 32 | $-(1+\alpha_3)z_{i-1jk} + 2(1+\alpha_1)z_{ijk} - (1-\alpha_3)z_{i+1jk}$ <br> $= (\alpha_1-\alpha_2)z_{ijk-1} + (\alpha_1+\alpha_2)z_{ijk+1} + \alpha_4$ | $\alpha_1 = \frac{d^2}{c_1^2},\ \alpha_2 = \frac{dd_{\psi*}}{2c_1^2},\ \alpha_3 = \frac{d_\phi}{2d},$ <br> $\alpha_4 = \frac{d_\phi(if)}{c_1 d} - \frac{(if)_\phi}{c_1} - \frac{d}{c_1^2}(fg)_{\psi*}$ |
| 33 | $-(1+\alpha_3)y_{i-1jk} + 2(1+\alpha_1)y_{ijk} - (1-\alpha_3)y_{i+1jk}$ <br> $= (\alpha_1-\alpha_2)y_{ijk-1} + (\alpha_1+\alpha_2)y_{ijk+1} + \alpha_4$ | $\alpha_1 = \frac{i^2}{c_1^2},\ \alpha_2 = \frac{ii_{\psi*}}{2c_1^2},\ \alpha_3 = \frac{i_\phi}{2i},$ <br> $\alpha_4 = \frac{i_\phi(gh)}{c_1 i} - \frac{(gh)_\phi}{c_1} - \frac{i(dh)_{\psi*}}{c_1^2}$ |
| 34 | $-(1+\alpha_3)z_{i-1jk} + 2(1+\alpha_1)z_{ijk} - (1-\alpha_3)z_{i+1jk}$ <br> $= (\alpha_1-\alpha_2)z_{ijk-1} + (\alpha_1+\alpha_2)z_{ijk+1} + \alpha_4$ | $\alpha_1 = \frac{i^2}{c_1^2},\ \alpha_2 = \frac{ii_{\psi*}}{2c_1^2},\ \alpha_3 = \frac{i_\phi}{2i},$ <br> $\alpha_4 = \frac{(dh)_\phi}{c_1} - \frac{i_\phi(dh)}{c_1 i} - \frac{i}{c_1^2}(gh)_{\psi*}$ |

cycle all tentative solutions for x, y, and z will be obtained as well as possibly tentative solutions for these variables on the boundary planes which are not of the Dirichlet type. The same process is repeated for the second cycle, etc. In the actual computer program as it has been written for the problem of flow around a strut, the additional capability has been provided to repeat all the tentative solutions for x, y, or z on interior planes more than one time before proceeding to the tentative solutions of the next variable.

The LSOR method has been used for the reasons given earlier to obtain all tentative solutions except for certain boundary planes as will be described later for the example problem which is given herein. While a description of the LSOR method can be found in a number of text books dealing with finite difference methods for PDE (see for example Ames, 1965), a brief explanation is given here for the sake of completeness as well as to point out certain unique features of the LSOR method as applied to the equations of Table 2.

The LSOR method can be understood by noting that the application of any of the operators in Table 2 across all interior grid points of a line leads to a system of linear algebraic equations provided that the α's and values on adjacent lines are known. In matrix notation this system has the form

$$A\vec{X} = \vec{B} \quad \ldots\ldots\ldots (44)$$

in which $\vec{X}$ represents the unknown vector, $\vec{B}$ is the vector of known quantities and A is a tridiagonal matrix. The fact that A is tridiagonal is an important feature of the method from a computational viewpoint, since such tridiagonal systems of equations can be solved by a single pass through the rows with a Guassian elimination which leaves a matrix with only two elements on each row; the diagonal element and the next element. The solution to the system is subsequently obtained by back substitution. Some writers have referred to the method for accomplishing this solution as the Thomas algorithm. This method defines the sequence of elements of A immediately to the left of, on, and immediately to the right of the diagonal by vectors $\vec{q}$, $\vec{r}$, and $\vec{s}$ respectively. Then additional elements of other vectors $\vec{f}$ and $\vec{g}$ are defined by

$$f_1 = \frac{s_1}{r_1},\ g_1 = \frac{b_1}{r_1}$$

$$f_m = \frac{s_m}{r_m - f_{m-1}q_m},\ g_m = f_m(b_m - q_m g_{m-1})/s_m \qquad 2 \le m \le n \quad \ldots (45)$$

in which n is the number of rows and columns in A, and the b's are the elements of $\vec{B}$. The solution vector $\vec{X}$ is obtained from

$$x_n = g_n$$

$$x_m = g_m - f_m x_{m+1} \qquad n-1 \ge m \ge 1 \quad \ldots (46)$$

In implementing the algorithm given by Eqs. 45 and 46 it is not necessary to set aside storage for a new array f. Rather, since the values of r need not be retained, the values of f may be stored in the former array positions for r.

Upon obtaining the solution vector $\vec{X}$ which represents the unknown values across an entire grid line, the individual elements are immediately adjusted by the over-relaxation formula

$$x_{ijk}^{p+1} = x_i + w_1(x_i - x_{ijk}^{p}) \quad \ldots\ldots (47)$$

in which the $x_i$'s (with the single subscript) are the elements of $\vec{X}$, and $x_{ijk}$ (with the triple subscript) are the values of the dependent variable x, y, or z at the grid points along the line in question. The superscript p represents the number of the iteration and $w_1$ is the over-relaxation factor with a value between zero and unity. Eq. 47 is not the usual form of the over-relaxation equation which utilizes an over-relaxation factor $w = w_1 + 1$. The use of Eq. 47 in place of the more usual form has the advantage that the computer core positions for the triple subscripted array $x_{ijk}$ needs to be located once instead of twice to carry out the arithmetic on the right of the equal sign.

The LSOR method proceeds from line to line until the value of the variables across all lines within the plane have been adjusted. Upon completing the last line the entire process is repeated as the next iteration, etc. In implementing the LSOR method for the equations in Table 2, the α's have been computed only during the first iteration and stored for subsequent iterations. The reason for doing this becomes obvious upon noting that some of the α's are independent of the solution on that plane, and those that are have minor effect on the resulting solution. Consequently, the majority of the arithmetic involved in solving the tridiagonal system repeatedly is with single real variables or single subscripted arrays. Since the α's will take on different values during the next cycle, particularly during the first few cycles of the solution process, there is no need to iterate until the tentative solution during first cycles satisfy a small error parameter. By permitting a limited number of iterations to occur in obtaining any tentative solution, the tentative solutions will progessively satisfy a smaller error parameter, until eventually during later cycles the specified error parameter will be satisfied with fewer than the maximum specified number of iterations.

# FREE SURFACE FLOW AROUND A STRUT

In the initial application of the previously described inverse solution to three-dimensional potential flows, a simple problem was selected to test the workability of the methods. The first such problem consisted of uniform flow in an open channel. After it was demonstrated that the methods did converge to the solution, providing a reasonable initialization was supplied to begin the process, the program used for a solution to this first test problem was modified to solve the problem of flow in a channel with vertical side walls past a vertical strut which extends through the free surface. This problem is described in detail herein. It demonstrates possible methods for incorporating boundary conditions into the solution of three-dimensional inversely formulated problems. While the problem represents what one might refer to as a "mildly three-dimensional problem," it does contain examples of the commonly encountered boundary conditions. Besides having the advantage that much of the flow behavior might be predicted from more elementary analyses, and therefore an indication of the adequacy of the methods may be evaluated, a "mildly three-dimensional problem" of this nature provides a base upon which a number of techniques for handling different boundary conditions can be experimented with and the best of the alternatives selected. It soon became apparent even while experimenting with the first problem of uniform channel flow, that completely satisfactory methods for handling free surfaces or cavity surfaces under the influence of gravity would be hard to come by. Hopefully, future research will improve upon some of the techniques described herein.

## Formulation and boundary conditions

A sketch of the problem of channel flow past a strut in the physical space is given in the upper portion of Fig. 1 and the same region in the $\phi\psi\psi^*$ space is given in the lower portion of this figure. The $\phi\psi\psi^*$ space has been selected such that the bottom of the channel defines the $\psi = 0$ stream surface and the top free surface of flow is defined by the $\phi\psi^*$ plane obtained by holding $\psi = M_1 = M\text{-}1$ where $M_1$ is the number of grid increments used in the finite difference solution in the $\psi$ direction. (Remember $\Delta\psi = 1$.) The plane $\phi\psi$ defined by $\psi^* = 0$ corresponds to the left wall of the channel (when facing downstream) and the right wall by $\psi^* = N_1 = N\text{-}1$. The beginning of the space boundary value problem through which the flow enters is assumed to be far enough upstream to be influenced insignificantly by the presence of the strut. This $\psi\psi^*$ plane is given by $\phi = 0$, and the last $\psi\psi^*$ plane of the $\phi\psi\psi^*$ boundary value problem is defined by $\phi = L_1 = L\text{-}1$.

After placing the problem in the $\phi\psi\psi^*$ space, the next step in the formulation consists of selecting the equations, from those in Table 1, to be used to solve for each of the three dependent variables x, y, and z. This selection should be based on consideration of the criteria given earlier. For the problem being considered here, the major component of velocity throughout all except small regions near the front and rear of the strut, is in the x-direction in the physical space. Furthermore because of the placing of the problem in the $\phi\psi\psi^*$ space, the channel bottom with $\psi = 0$ is normal to the y-direction and the sides of the channel with $\psi^*$ held constant are normal to the z-direction. Consequently, greater variation of x occurs in $\phi\psi$ or $\phi\psi^*$ planes, than in $\psi\psi^*$ planes. The major change in y is in the $\psi$-direction. Therefore, a plane defined by $\psi$ as one coordinate should be selected for obtaining the solutions for y. Likewise, the major variation of z is in the direction of $\psi^*$, and consequently z would be fairly constant on separate $\phi\psi$ planes.

Therefore, the first criteria stated earlier, namely that the assumption of knowns be as valid as possible, would suggest that x could be solved for on separate $\phi\psi$ or $\phi\psi^*$ planes, but not $\psi\psi^*$ planes. Clearly the magnitude of $x_\phi$ is larger than $x_\psi$ or $x_{\psi^*}$ in general and consequently an easily generated initialization of the problem would have larger errors in the magnitudes of $x_\phi$, than $x_\psi$ or $x_{\psi^*}$.

The second criteria, namely that the coefficients of the two second derivatives have nearly equal magnitudes, will be used to narrow the choice down further. For x on $\phi\psi$ or $\phi\psi^*$ planes the available equations are 23, 25, 29, and 31. In comparing the magnitudes of coefficients of second derivatives $c_1$ may be compared to the square of the single letters representing the derivative, i.e. with $e^2$, $f^2$, $g^2$, and $d^2$. Should the problem be specified so that the magnitude of $c_1$ is close to unity, as will be the case, then either Eq. 23 or 31 could be selected. Equations 25 and 29 are eliminated because the coefficients $f = y_{\psi^*}$ and $g = z_\psi$ are much smaller whereas $e = z_{\psi^*}$, and $d = y_\psi$ are close to unity in magnitude. The final selection between Eq. 23 or 31 is arbitrary. In solving the problem, Eq. 23 has been used.

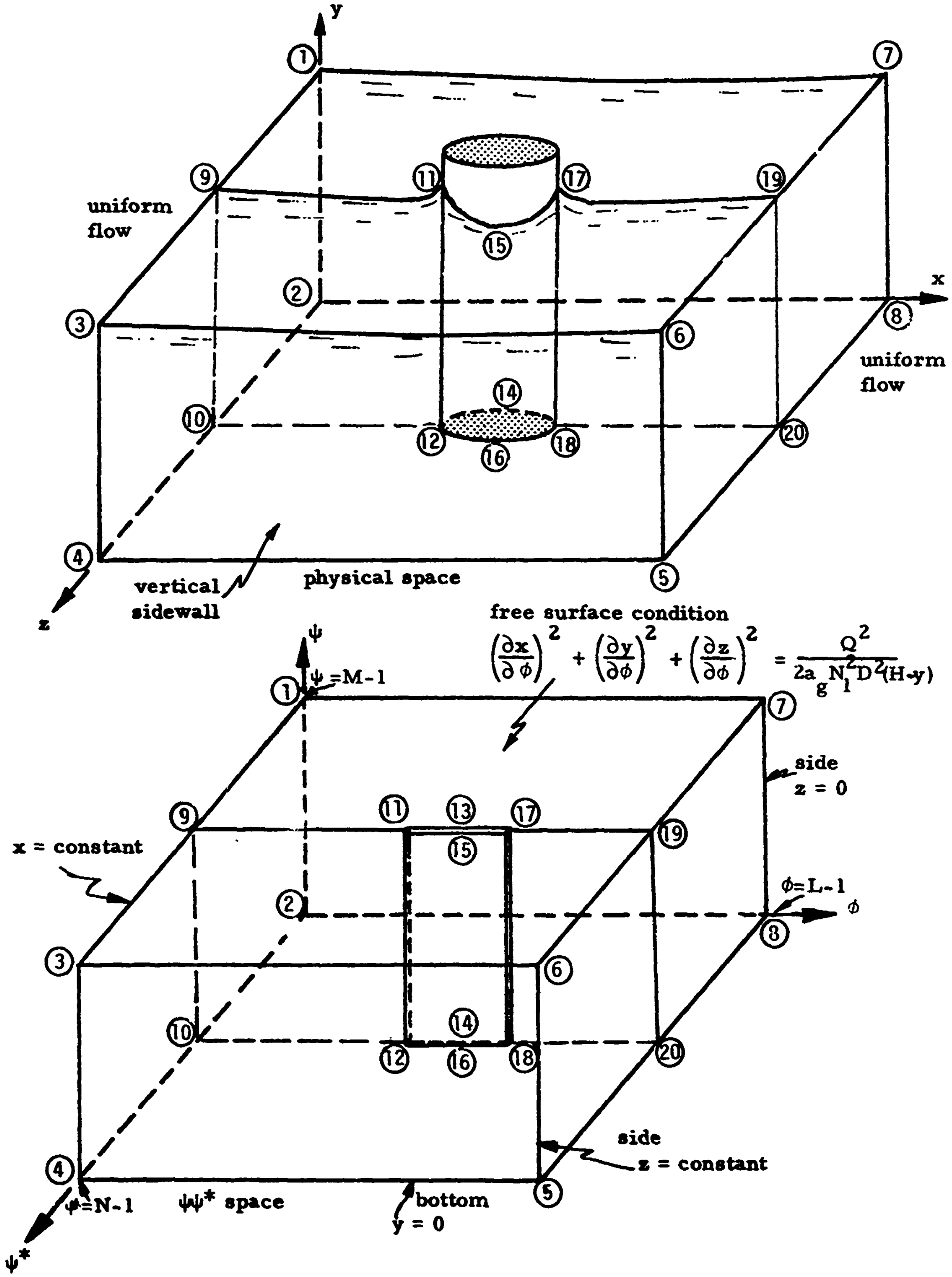


Fig. 1. Schematic diagrams in the physical and φψψ* space of flow with a free surface past a vertical strut.

The equation to use in solving for y is between 24 and 27 in $\phi\psi$ planes. Since the magnitude of $h = x_{\psi^*}$ is much smaller in general for this problem than $c_1$, Eq. 24 will be used to obtain the tentative solutions for y.

For obtaining solutions for z only the two equations 30 and 34 on $\phi\psi^*$ planes will be considered further. Of these two equations, 34 is eliminated since the coefficient $i = x_\psi$ is small and the coefficient $d = y_\psi$ in Eq. 30 is close to unity. In summary the tentative solutions for x and y will be obtained from separate $\phi\psi$ planes. Equation 23 will be used for x and Eq. 24 for y. The tentative solutions for z will be by means of Eq. 32 on $\phi\psi^*$ planes.

Using the above description of the $\phi\psi\psi^*$ space and the selected equations, the boundary conditions given below can be developed. Some of these conditions are also shown in the lower portion of Fig. 1 to help identify that boundary and its condition in the $\phi\psi\psi^*$ space. A description of how these boundary condition equations are obtained follows the listing of the equations.

a. *Bottom* 2, 10, 4, 5, 20, 8

$$y(\phi, 0, \psi^*) = 0 \quad \ldots\ldots\ldots\ldots (48)$$

$$x(\phi, 0, \psi^*) = \frac{1}{c_1}\int_{\psi\psi^*} \left(\frac{\partial y}{\partial \psi}\right)\left(\frac{\partial z}{\partial \psi^*}\right) d\phi \quad \ldots (49)$$

$$z_{\phi\phi} + \frac{d^2}{c_1^{\,2}} z_{\psi^*\psi^*} + \frac{dd_{\psi^*}}{c_1^{\,2}} z_{\psi^*} - \frac{d_\phi}{d} z_\phi = 0 \quad \ldots (50)$$

b. *Left Side* 1, 2, 7, 8

$$z(\phi, \psi, 0) = 0 \quad \ldots\ldots\ldots\ldots (51)$$

$$x_{\phi\phi} + \frac{e^2}{c_1^{\,2}} x_{\psi\psi} + \frac{ee_\psi}{c_1^{\,2}} x_\psi - \frac{e_\phi}{e} x_\phi = 0 \quad \ldots (52)$$

$$y_{\phi\phi} + \frac{e^2}{c_1^{\,2}} y_{\psi\psi} + \frac{ee_\psi}{c_1^{\,2}} y_\psi - \frac{e_\phi}{e} y_\phi = 0 \quad \ldots (53)$$

c. *Right Side* 3, 4, 5, 6

$$z(\phi, \psi, N_1) = \text{constant} \quad \ldots\ldots\ldots (54)$$

for x the same as Eq. 52
for y the same as Eq. 53

d. *Upstream Entrance* 1, 2, 10, 4, 3, 9

$$x(0, \psi, \psi^*) = 0 \quad \ldots\ldots\ldots\ldots (55)$$

$$y(0, \psi, \psi^*) = \frac{\psi}{M_1} H \quad \ldots\ldots\ldots (56)$$

$$z(0, \psi, \psi^*) = \frac{\psi^*}{M_1} H \quad \ldots\ldots\ldots (57)$$

e. *Downstream Exit* 7, 8, 20, 5, 6, 19

$$x(L_1, \psi, \psi^*) = \text{constant} \quad \ldots\ldots\ldots (58)$$

for y the same as Eq. 56
for z the same as Eq. 57

f. *Free Surface* 1, 7, 19, 6, 3, 9

$$(g^2 + i^2)\left(\frac{\partial y}{\partial \psi^*}\right)^2 - 2\frac{\partial y}{\partial \psi}(eg + ih)\frac{\partial y}{\partial \psi^*} + (e^2 + h^2)\left(\frac{\partial y}{\partial \psi}\right)^2 + c_1^{\,2}\left(\frac{\partial y}{\partial \phi}\right)^2 - \frac{Q^2}{2a_g N_1^2 D^2 (H-y)} = 0 \quad \ldots (59)$$

$$x(\phi, M_1, \psi^*) = \int_{\psi\psi^*} \sqrt{\frac{Q^2}{N_1^2 D^2 (2a_g)(H-y)} - \left(\frac{\partial y}{\partial \phi}\right)^2 - \left(\frac{\partial z}{\partial \phi}\right)^2}\, d\phi \quad \ldots (60)$$

$$z = \int_{\phi\psi} \frac{c_1 \frac{\partial x}{\partial \phi} + \frac{\partial y}{\partial \psi^*}\frac{\partial z}{\partial \psi}}{\partial y/\partial \psi}\, d\psi^* \quad \ldots (61)$$

g. *Left Side of Strut* 11, 13, 17, 18, 14, 12

$$z(\phi, \psi, NS) = f(\phi) \text{ specified by input} \quad \ldots (62)$$

$$x_{\phi\phi} + \frac{e^2}{c_1^{\,2}} x_{\psi\psi} + \frac{ee_\psi}{c_1^{\,2}} x_\psi - \frac{e_\phi}{e} x_\phi = 0 \quad \ldots (63)$$

$$y_{\phi\phi} + \frac{e^2}{c_1^{\,2}} y_{\psi\psi} + \frac{ee_\psi}{c_1^{\,2}} y_\psi - \frac{e_\phi}{e} y_\phi = 0 \quad \ldots (64)$$

h. *Right Side of Strut* 11, 15, 17, 18, 16, 12

for z, x, and y the same as Eqs. 62, 63, and 64

A number of the boundary conditions just given are immediately obvious. The equations for other boundary conditions result only after some algebraic manipulation. For these latter conditions an explanation and the derivation of the given equation are contained below.

The condition for x along the channel bottom has been obtained from Eq. 20 by noting that since y = 0 (constant) along this boundary $y_{\psi^*} = 0$. Therefore,

$$c_1 x_\phi = y_\psi z_{\psi^*} \quad \ldots\ldots\ldots\ldots (49a)$$

Integrating Eq. 49a with $\psi$ and $\psi^*$ both held constant gives Eq. 49 in which the subscripts to the integral sign denotes that $\psi$ and $\psi^*$ are to be held

constant. Since $\psi$ is constant along the bottom, the integration of Eq. 49 becomes a numerical line integration along the bottom $\psi^* =$ constant grid lines with $\phi$ being incremented. The implementation of this line integration involves the two step procedure of first evaluating the two partial derivatives with the integral, and secondly carrying out the numerical integration. The evaluation of $y_\psi$ has been based on up through third order forward differences and is given by

$$\left.\frac{\partial y}{\partial \psi}\right|_{j=1} \approx \frac{1}{\Delta\psi}\left[3y_{i2k} - \frac{11}{6}y_{i1k} - \frac{3}{2}y_{i3k} + \frac{1}{3}y_{i4k}\right] \ldots (65)$$

The evaluation of $z_{\psi^*}$ has been based on third order forward, fourth order central, or third order backward differences respectively depending upon whether $\psi^* = 0$, $\psi^* = \Delta\psi^*$, whether $\psi^*$ lies within the central portion of the bottom, or whether $\psi^* = N_1$, or $\psi^* = M_1 - \Delta\psi^*$. For $\psi^* = 0$ (i.e. k = 1) the equation is

$$\left.\frac{\partial z}{\partial \psi^*}\right|_{k=1} \approx \frac{1}{\Delta\psi^*}\left[3z_{i1,2} - \frac{11}{6}z_{i1,1} - \frac{3}{2}z_{i1,3} + \frac{1}{3}z_{i1,4}\right] \ldots\ldots\ldots\ldots (66)$$

The equation for $\psi^* = \Delta\psi^* = 1$ is

$$\left.\frac{\partial z}{\partial \psi^*}\right|_{k=2} \approx \frac{1}{\Delta\psi^*}\left[z_{i1,3} - \frac{1}{3}z_{i1,1} - \frac{1}{2}z_{i1,2} - \frac{1}{6}z_{i1,4}\right] \ldots\ldots\ldots\ldots (67)$$

For the central portion (i.e. k = 3, 4, ..., N-2)

$$\left.\frac{\partial z}{\partial \psi^*}\right|_{k} \approx \frac{1}{\Delta\psi^*}\left[\frac{2}{3}(z_{i1k+1} - z_{i1k-1}) - \frac{1}{12}(z_{i1k+2} - z_{i1k-2}\right] \ldots\ldots\ldots\ldots (68)$$

Equations similar to Eqs. 67 and 68 but based on backward differences apply along the lines $\psi^* = N_1$ (k = N) and $\psi^* = N_1 - \Delta\psi^*$ (k = N-1).

The numerical integration, for other than the first interval $\phi = 0$ to $\phi = \Delta\phi = 1$ or the final interval $\phi = L_1 - \Delta\phi$ to $\phi = L_1$ has been based on Bessel's interpolation formula for a third degree polynomial passing through the values of four consecutive values of the arguments given by the product of the two derivatives $y_\psi$ and $z_{\psi^*}$. This integration formula is

$$\Delta x = \Delta\phi\left[\frac{13}{24}\left(y_\psi z_{\psi^*}\big|_i + y_\psi z_{\psi^*}\big|_{i+1}\right) - \frac{1}{24}\left(y_\psi z_{\psi^*}\big|_{i-1} + y_\psi z_{\psi^*}\big|_{i+2}\right)\right] \ldots (69)$$

Across the first and final intervals this integration has been based on the trapezoidal formula,

$$\Delta x = \frac{\Delta\phi}{2}\left[y_\psi z_{\psi^*}\big|_i + y_\psi z_{\psi^*}\big|_{i+1}\right] \ldots\ldots\ldots (70)$$

in which i = 1 or i = L-1.

The other boundary conditions, Eqs. 60 and 61, which contain integrals as in Eq. 49 have been handled in the same general manner. Individual details differ in each case, but the derivatives involved in the particular equation have been approximated by third order forward or backward difference and fourth order central difference in the interior wherever possible. The integration has been based on a polynomial passing through values equal to four derivatives or products, etc., thereof, except over the first and last intervals of the line integration which has been based on the trapezoidal rule. If the final value of the integrated variable is known upon reaching the opposite boundary (as with z from Eq. 61 on the free surface) any error in not closing on this correct value is proportioned according to the distance from the beginning point. In the case of x on the bottom and the free surface (Eqs. 49 and 60) the average of all final values is obtained and then the individual differences from this average are distributed according to the magnitude of x.

The boundary condition for z along the bottom, Eq. 50, has been obtained from Eq. 32 by noting that $f = y_{\psi^*} = 0$ and consequently Eq. 32 reduces to Eq. 50.

The finite difference operator for Eq. 50 is:

$$-(1+\alpha_3)z_{i-1,1k} + 2(1+\alpha_1)z_{i1k} - (1-\alpha_3)z_{i+1,1k} = (\alpha_1 - \alpha_2)z_{i1k-1} + (\alpha_1 + \alpha_2)z_{i1k+1} \ldots (71)$$

in which

$$\alpha_1 = (y_\psi)^2/c_1 = (y_{i2k} - y_{i1k})^2/c_1$$

$$\alpha_2 = \frac{1}{2}y_\psi y_{\psi\psi^*}/c_1 = \frac{1}{4}(y_{i2k} - y_{i1k})(y_{i2k+1} - y_{i1k+1} - y_{i2k-1} + y_{i1k-1})/c_1$$

$$\alpha_3 = \frac{1}{2}y_{\phi\psi}/y_\psi = \frac{1}{4}(y_{i+1,2k} - y_{i+1,2k} - y_{i-1,2k} + y_{i-1,2k})/(y_{i2k} - y_{i1k})$$

The boundary condition Eqs. 52 and 53 which apply for x and y respectively on the two sides of the channel are obtained from Eqs. 23 and 24 by noting that z is constant in the $\phi\psi$ planes of the channel sides and

consequently $g = z_\psi = 0$ and $c = z_\phi = 0$. The finite difference operators for Eqs. 52 and 53 are respectively

$$(1+\alpha_3)x_{i-1jk_1} + 2(1+\alpha_1)x_{ijk_1} - (1-\alpha_3)x_{i+1jk_1}$$
$$= (\alpha_1 - \alpha_2)x_{ij-1k_1} + (\alpha_1 + \alpha_2)x_{ij+1k_1} \quad . . (72)$$

and

$$(1+\alpha_3)y_{i-1jk_1} + 2(1+\alpha_1)y_{ijk} - (1-\alpha_3)y_{i+1jk}$$
$$= (\alpha_1 - \alpha_2)y_{ij-1k_1} + (\alpha_1 + \alpha_2)y_{ij+1k_1} \quad . . (73)$$

in which

$$\alpha_1 = \frac{e^2}{c_1^2} = (z_{ijk_1} - z_{ijk_2})^2/c_1^2$$

$$\alpha_2 = \frac{e}{2c_1^2} e_\psi = \frac{1}{8}(z_{ijk_1} - z_{ijk_2})(z_{ij+1k_1} - z_{ij-1k_1} + z_{ij-1k_2})/c_1^2$$

$$\alpha_3 = \frac{e_\phi}{2e} = \frac{1}{4}(z_{i+1jk_1} - z_{i+1jk_2} - z_{i-1jk_1} + z_{i-1jk_2})/(z_{ijk_1} - z_{ijk_2})$$

and the subscripts $k_1 = 1, k_2 = 2$ on the left side and $k_1 = N, k_2 = N\text{-}1$ on the right side of the channel.

At the upstream entrance the boundary conditions have been obtained under the assumption that the flow is uniform. The value of x is therefore constant and assigned the value of zero, and the difference in z's between consecutive $\psi^*$ constant grid lines on the face equals the difference in y's between consecutive $\psi$ constant grid lines. The width of channel is therefore specified in relationship to the depth of flow by the equation

$$W = \frac{N_1}{M_1} H \quad . . . . . . . . . . . . . . . . (74)$$

The assumption of uniform flow is also made at the downstream final face. Therefore the conditions are the same as at the upstream face except that x becomes the constant equal to the average of the x's obtained from the numerical integrations of Eqs. 49 and 60 on the bottom and free surface respectively.

The shape of the strut has been specified by giving the z coordinates of both sides along a specified $\psi^*$ constant line. In the example solution given later this $\psi^*$ constant line has been selected midway between the two channel sides, and the z's have been specified for each potential surface intersecting with both sides of the strut to result in symmetry about the center plane of the channel. This simplified problem could actually have been solved using only 1/2 of the $\phi\psi\psi^*$ space. The full problem was used primarily to examine the performance of the solution technique in duplicating the symmetry which must exist. For a nonsymmetry problem, the specification of the shape of the strut could be given by changes of z from that at the stagnation $\psi^*$ equal constant line at the front of the strut.

The boundary conditions, Eqs. 63 and 64, for x and y on the sides of the strut are obtained by noting that z is only a function of $\phi$ but constant with variation of $\psi$. Consequently $g = z_\psi = 0$, and Eqs. 23 and 24 reduce to Eqs. 63 and 64, just as they reduced to Eqs. 52 and 53 for the boundary conditions on the channel sides. Since Eqs. 63 and 64 are identical to Eqs. 52 and 53, the finite difference operators for x and y along the strut are identical to Eqs. 72 and 73 with $k_1$ and $k_2$ equal to NS and NS-1 respectively along the left side of the strut and $k_1$ = NS, $k_2$ = NS+1 on the right side of the strut.

**Free surface boundary conditions**

The implementation of the previously discussed boundary conditions has been relatively straight forward. This has not been the case with the conditions on the free surface, and consequently the free surface conditions and the difficulties encountered in implementing them will be discussed in this section.

The free surface is at atmospheric pressure and consequently the sum of the velocity head and the magnitude of y at any point on the surface must equal a constant $H_g$, i.e.

$$y + \frac{V^2}{2a_g} = H \quad . . . . . . . . . . . . . . . (74)$$

in which $a_g$ is the acceleration of gravity. The magnitude of the velocity squared can be expressed in terms of the inverse variables by substituting each of the first equations in Eqs. 6, 7, and 8 into the middle portions of Eqs. 1, 2, and 3 respectively to give,

$$V^2 = u^2 + v^2 + w^2 = J^2 [x_\phi^2 + y_\phi^2 + z_\phi^2] \quad . . . . (75)$$

But from the definition of J below Eq. 6 it can be shown that $J = V^2$, therefore Eq. 75 reduces to,

$$V^2 = \frac{1}{x_\phi^2 + y_\phi^2 + z_\phi^2} \quad . . . . . . . . . . . (76)$$

Upon combining Eqs. 76 and 74 and transforming the resulting equation by Eq. 17 to introduce the dimensionless dependent variable $\phi$ leads to the following basic free surface boundary condition.

$$x_\phi^2 + y_\phi^2 + z_\phi^2 = \frac{Q^2}{2a_g N_1^2 D^2 (H - y)} \quad \ldots\ldots (77)$$

A number of alternative schemes for use of Eq. 77 in the finite difference solution for establishing the values of x. y and z on the free surface have been investigated by implementing them in computer algorithm and then examining their performance. All of the schemes which have been investigated are associated with a number of numerical difficulties and it appears that successful solutions can be obtained only if the computational procedures anticipate and avoid these potential difficulties.

The first scheme implemented developed the finite difference operator for y on the free surface by replacing the first term in Eq. 77 by its equivalent from Eq. 20 and assumed the third term might be considered the known c $= z_\phi$. The derivatives in the resulting equation were then approximated by second order central differences. The value $y_{im+1,k}$ at the nonexistent grid point in this difference equation was eliminated by combining the equation with the operator Eq. 24 for y at interior grid points to give the operator,

$$\begin{aligned} f = &- (1+\alpha_3) y_{i-1mk} + 2(1+\alpha_1) y_{imk} - (1-\alpha_3)_{i+1mk} \\ &- 2\alpha_1 y_{im-1k} - \frac{(\alpha_1+\alpha_2)}{e} \left[ 2fg + \right. \\ &\left. {}^{-1}\sqrt{\frac{2Q^2}{N_1^2 D^2 a_g (H - y_{imk})} - (z_{i+1mk} - z_{i-1mk})^2 - (y_{i+1mk} - y_{i-1mk})^2} \right] \\ &- \alpha_4 = 0 \quad \ldots\ldots\ldots\ldots (78) \end{aligned}$$

in which the α's are as defined in Table 2 for Eq. 24.

Note that, Eq. 78 cannot be solved explicitly for $y_{imk}$ even under the assumption that the derivatives given by the single letters are known as is the case with the other operator in Table 2. Consequently in applying Eq. 78 at consecutive grid points along the line defined by incrementing i in the LSOR method a system of nonlinear algebraic equations results. This nonlinear system has been solved by the generalized Newton iterative method,

$$\vec{y}^{(q+1)} = \vec{y}^{(q)} - D^{-1} \vec{f}^{(q)} \quad \ldots\ldots\ldots (79)$$

in which $\vec{y}$ is the vector of unknowns $y_{imk}$, i = 1, 2, ... L, the superscript q denotes iteration number, the vector f has as its elements the values obtained by applying Eq. 78 at the individual grid points, and D is the commonly defined Jacobian derivative determinant.

$$D = \begin{vmatrix} \frac{\partial f_1}{\partial y_1} & \frac{\partial f_1}{\partial y_2} & \cdots & \frac{\partial f_1}{\partial y_n} \\ \vdots & & & \\ \frac{\partial f_n}{\partial y_1} & \cdots & \cdots & \frac{\partial f_n}{\partial y_n} \end{vmatrix}$$

Since the determinant D is tridiagonal for the system of equations obtained from Eq. 78, and since $D^{-1}\vec{f}$ represents the solution to a system $Dx = \vec{f}$, the same algorithm used for solving the other operators in the LSOR method can be utilized. The difference is that the algorithm must be repeated for each iteration in obtaining the solution across any line.

In studying the performance of this approach it soon became evident that it required a very good initialization of values if it were to give correct values for y on the free surface. Not only did it require a close initialization of surface values, but the interior values had to be well settled by their operators before the free surface values were adjusted. Much could be written about why this is necessary, but perhaps the best means for illustrating why good initialization is critical to prevent the free surface values from straying too far from their correct values during the process of obtaining a finite difference solution is by graphs. Figures 2A through 2S show the variation of the function f defined by Eq. 78 over a relatively small range of $y_{imk}$. In each case H was equal to 10.5 and the remaining values in Eq. 78 (with the exception of perhaps one) were assigned the correct values for uniform flow with a depth y = 10. Figure 2A shows f vs. $y_{imk}$ with all other values correct, and as expected f is zero when $y_{imk} = 10$. However, an additional zero of f exists for a slightly larger value of $y_{imk}$ also. Obvious numerical difficulties would result if the incorrect second zero for f were selected during the iterative solution process.

More critical, however, is the behavior of the function with small changes of the other variables in the equation. The remaining curves in Figs. 2 show the variation of f with $y_{imk}$ with one of the other dependent variables x, y, or z at an adjacent grid point set to a value ± 0.15 from its correct values. As the value $y_{i+1mk}$ decreases slightly from its correct value (see Fig. 2B), it causes the first zero of f to correspond to a value of $y_{imk}$ less than 10 as one would expect and the second zero to become further removed from the first. With an increase in $y_{i+1mk}$, however, the two zeros became closer together. and for the increase of 0.15 used in Fig. 2C to almost coincide. Clearly a larger error would cause no real zero to exist for the function at least in the vicinity of the value $y_{imk}$ needed for a correct solution. When this situation occurs, the Newton method would project off far from the value being sought. This grossly erroneous value in turn affects adjacent functions with the result that the Newton method never returns during subsequent iterations with reasonable values of $y_{imk}$.

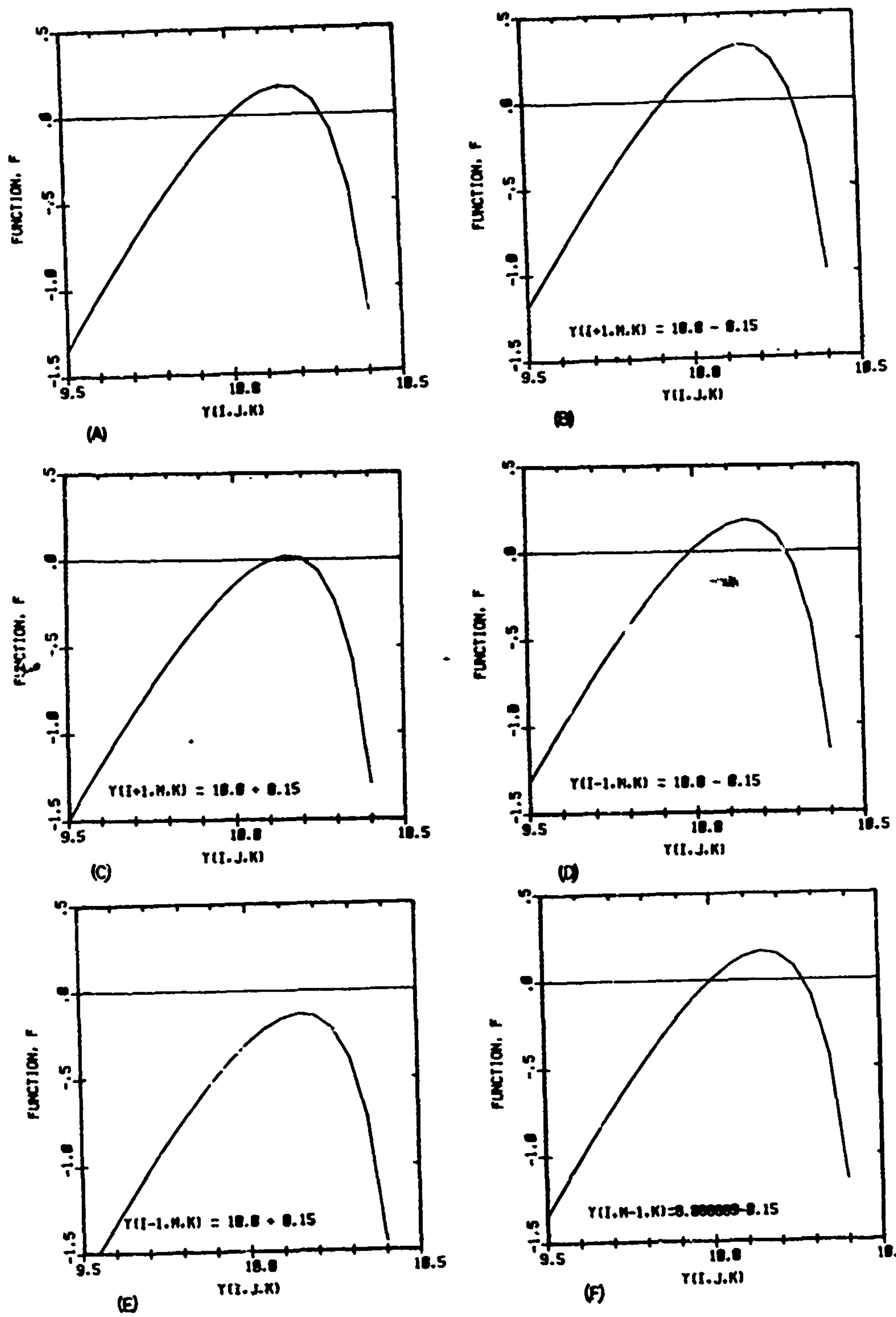


Fig. 2. Variation of the finite difference function given by Eq. 78 over a small range of $y_{imk}$ with no error (A), or a small error at several surrounding grid points (B-S).

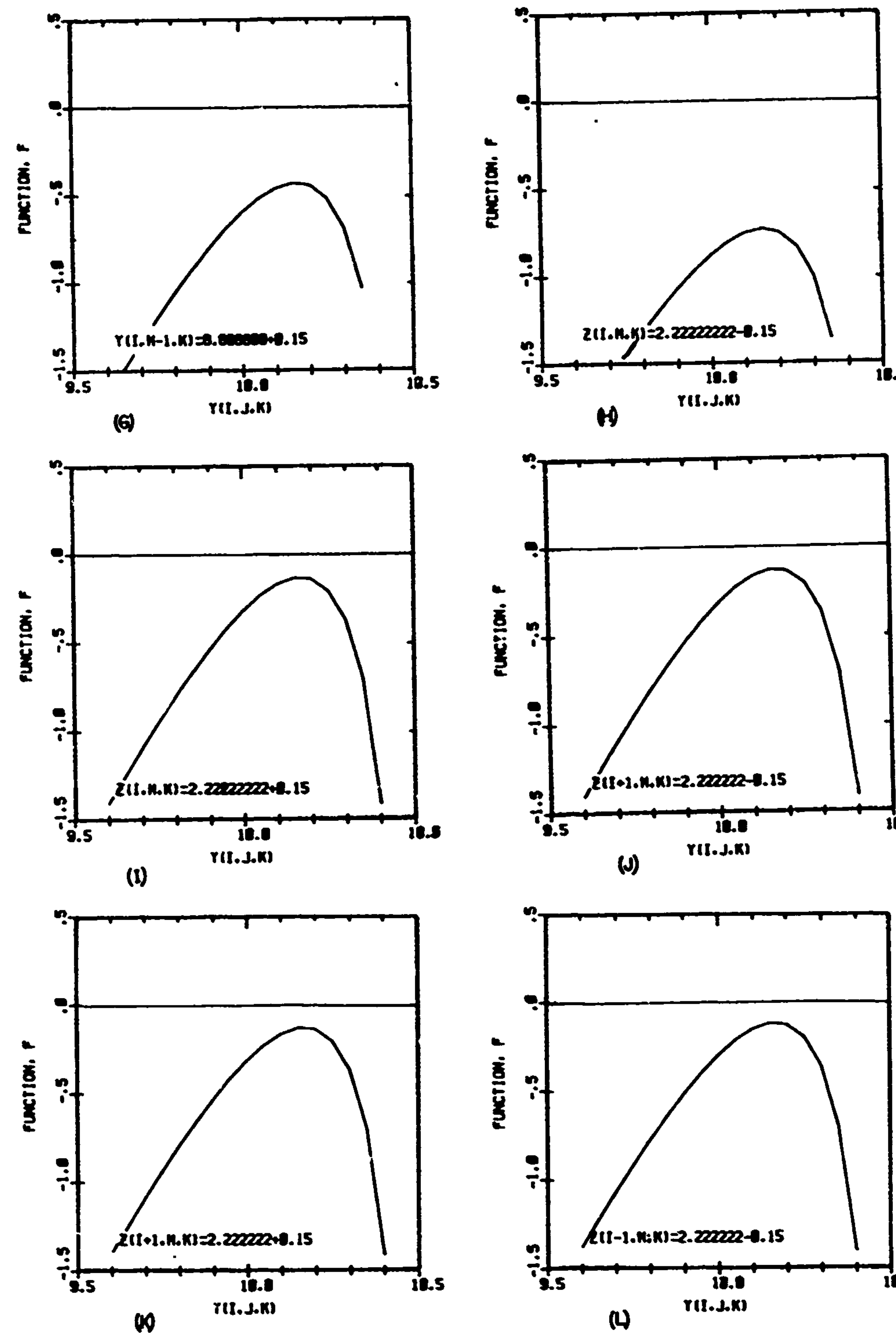


Fig. 2. Continued.

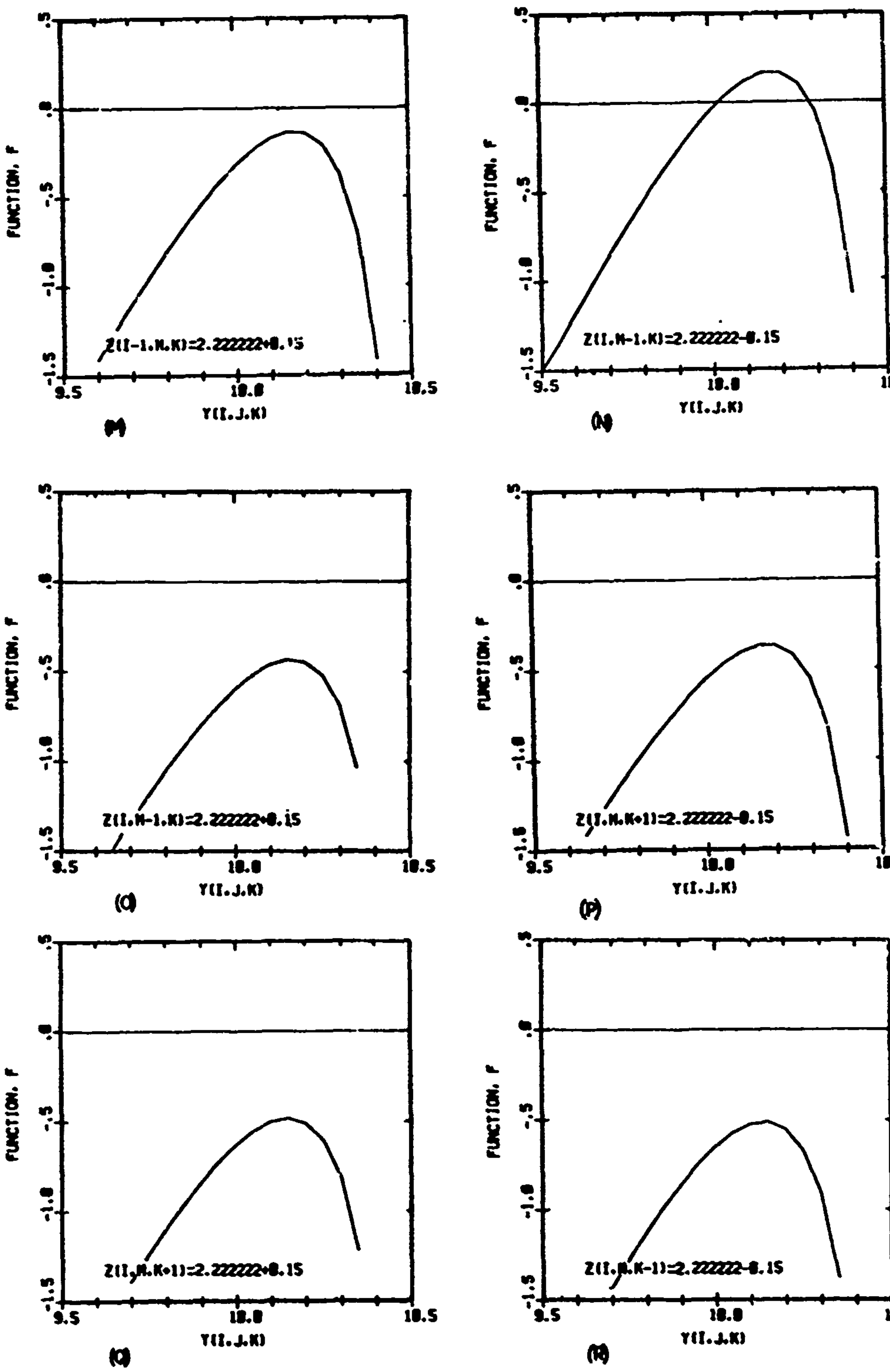


**Fig. 2. Continued.**

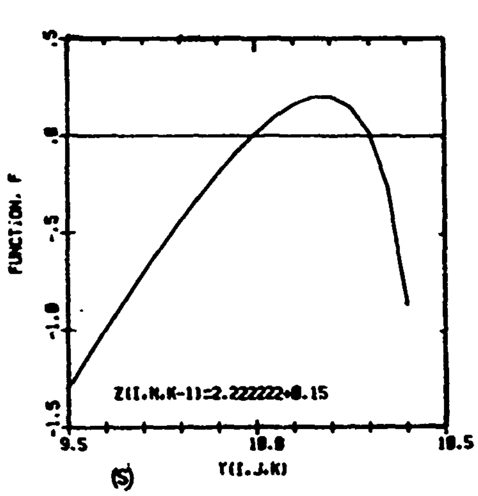


Fig. 2. Continued.

Decreasing or increasing the other values of x, y, or z at surrounding grid points, or x and z at that free surface grid point, cause similar behavior in f as can be noted by the remaining curves in Figs. 2. For the small errors of $\pm$ 0.15 used in plotting Figs. 2 the function f has lost its real zeros in 12 of the 19 cases shown.

An operator for x developed in much the same manner as Eq. 78, except that the second term in Eq. 77 was replaced by its equivalent from Eq. 21, and the result combined with Eq. 24, was also studied. It w . hoped that since the $y_{imk}$ which appears in Eq. 78 and also appears in the finite difference operator for x, but in the x operator it is considered known, that the implementation of the operator for x would be associated with fewer problems. However, as with the y operator convergence was obtained by the Newton-LSOR methods combined, only if the initialization was very good.

Similar problems exist for an operator for z obtained by combining the finite difference expression from forms of Eqs. 77 with the regular z operator. It has therefore been concluded that the difficulties discussed above are an inherent part of the free surface boundary condition Eq. 77 which cannot be eliminated by some manipulation of the available equations. At least no such manipulation is obvious. It was decided, therefore, that programming techniques would have to be adopted that would prevent the difficulties from occurring as far as this was practical, and that means would have to be included in the program to handle the difficulties when they did occur.

The approach for handling the free surface boundary conditions for x and z was, therefore, based on the integral Eqs. 60 and 61, and Eq. 59 was used for y on the free surface to incorporate the basic condition Eq. 77 which must be satisfied. In implementing Eq. 59 for y it was decided that its finite difference equivalent should be satisfied on a point by point basis, rather than over an entire line at a time, because of the difficulties associated with coping with vanishing zeros of the function.

The boundary condition Eq. 59 for y on the free surface is obtained by substituting for $x_\phi$ and $z_\phi$ from Eqs. 20 and 22 into Eq. 77. The finite difference operator for y on the free surface has been obtained by replacing the derivatives in Eq. 59 by second order or higher order differences. For those grid points with k = 2, k = N, or i = 2, the operator will be different than at the interior point on this boundary because of the need to use non-symmetric differences to approximate $y_{\psi*}$. For interior free surface boundary grid points the operator is

$$
\begin{aligned}
f = {} & (g^2+i^2)\left[\frac{1}{6}y_{imk-2} - y_{imk-1} + \frac{1}{2}y_{imk} + \frac{1}{3}y_{imk*}\right]^2 \\
& + \left[1.5y_{imk} - 2y_{im-1k} + .5\,y_{im-2k}\right]^2 (e^2+h^2) \\
& - \left[1.5y_{imk} - 2y_{im-1k} + .5y_{im-2k}\right]\left[2(eg+ih)\right] \\
& \left[\left(\frac{1}{6}y_{imk-2} - y_{imk-1} + \frac{1}{2}y_{imk} + \frac{1}{3}y_{imk+1}\right)\right] \\
& + c_1^2\left(\frac{1}{6}y_{i-2mk} - y_{i-1mk} + \frac{1}{2}y_{imk} + \frac{1}{3}y_{i+1mk}\right)^2 \\
& - \frac{Q^2}{2gN_1^2D^2(H-y_{imk})} = 0 \qquad \text{. . . . . . . . .(80)}
\end{aligned}
$$

For grid points along the grid line with k = 2, the quantity within the first square brackets has been replaced by the following third order difference approximation

$$y_{\psi*}\Big|_{k=2} = y_{im3} - \frac{1}{3}y_{im1} - \frac{1}{2}y_{im2} - \frac{1}{6}y_{im4} \quad \text{. . .(81)}$$

and for the grid line i = 2. Similar changes are necessary in the second from the final term in Eq. 80.

Before describing how Eq. 80 has been solved to overcome the difficulties associated with the vanishing of the real zeros and dual zeros of the previous operator f of Eq. 78, it is well to point out some characteristics of Eq. 80. First note that Eq. 80 is also implicit in $y_{imk}$ and therefore the solution to Eq. 80 must be obtained by an iterative method. Plots showing the variation of f of Eq. 80 with $y_{imk}$ for small errors in some of the surrounding points are given in Fig. 3. These graphs indicate the following:

1. The zero being sought is always associated with the smaller of the two possible values of $y_{imk}$ which lie within the vicinity of the solution being sought. (While the smaller $y_{imk}$ is sought for the formulation given earlier in this report, it does not indicate this will always be so. It was discovered that if both the dependent and independent variables are made dimensionless, then the larger of these two possible roots is the correct one.)

2. The function has a positive derivative with respect to $y_{imk}$ at the point of the correct zero if this zero exists.

3. The function has a negative derivative with respect to $y_{imk}$ at the point of the incorrect zero.

4. If real zeros of the function vanish, then $y_{imk}$ associated with the minimum absolute value of the function (or the minimum of the function squared) is not too different from the value of $y_{imk}$ which is being sought, and which will again come into existence when the errors in the variables at the surrounding grid points are eliminated.

Based on these observations, the solution to Eq. 80 at each grid point on the free surface proceeds at first by computing both f and its derivative based on the current value of $y_{imk}$ and also for a value $y_{imk} + \Delta y$, in which $\Delta y$ is small, i.e. $\Delta y = .005$. The derivative of f is given by:

$$
\begin{aligned}
\frac{\partial f}{\partial y_{imk}} = {} & 3(e^2 + h^2)(1.5 y_{imk} - 2 y_{im-1k} + .5 y_{im-2k}) \\
& - \frac{Q^2}{2 a_g N_1 M_1^2 (H - y)^2} + c_1^2 \left(\frac{1}{6} y_{i-2mk} - y_{i-1mk}\right. \\
& \left. + \frac{1}{2} y_{imk} + \frac{1}{3} y_{i+1mk}\right) + [(g^2 + i^2) \\
& - 3(eg + ih)] \left(\frac{1}{6} y_{imk-2} - y_{imk-1} + \frac{1}{2} y_{imk}\right. \\
& \left. + \frac{1}{3} y_{imk+1}\right) - (eg + ih)(1.5 y_{imk} - 2 y_{im-1k} \\
& + .5 y_{im-2k} \quad \ldots\ldots\ldots\ldots \quad (82)
\end{aligned}
$$

(It is necessary to modify Eq. 82 slightly for grid points adjacent to the boundaries, i.e. for $k = 2$, $k = N-2$, and $i = 2$.)

Should the derivative associated with $y_{imk}$ be negative (obviously the other derivative associated with $y_{imk} + \Delta y$ will also be negative), then $y_{imk}$ is decreased by a small amount (in the order of .005) and the procedure is begun again. If upon repeating this process of decreasing $y_{imk}$ the first derivative becomes positive and the second remains negative and both of the functions are still negative then no real root exists (or if it did exist two zeros would lie between $y_{imk}$ and $y_{imk} + .005$) and the solution proceeds by calling on an algorithm which uses the Fibonacci search technique (Wilde and Beighter, 1967) to find the $y_{imk}$ associated the minimum value of $f^2$ within the interval $y_{imk}$ to $y_{imk} + .005$.

Should, on the other hand, the first computation for f be positive and the derivative $\partial f / \partial y$ also be positive then $y_{imk}$ is decreased in value until f associated with $y_{imk}$ becomes negative and f associated with $y_{imk} + .005$ is still positive. As soon as this occurs the Newton method

$$
y_{imk}^{(p+1)} = y_{imk}^{(p)} - \frac{f^{(p)}}{\frac{df}{dy}} \quad \ldots\ldots\ldots \quad (83)
$$

or the False-Position method is used to find the zero of f.

The remaining possibility is that the value of f associated with $y_{imk}$ is negative (its derivative positive), but f associated with $y_{imk} + .005$ is also negative. Should this be the case then $y_{imk}$ is increased in value by a small amount and the computation repeated until one of the cases above has occurred, and the smaller $y_{imk}$ giving a zero f has been obtained or the $y_{imk}$ associated with the minimum value of $f^2$ has been found by the Fibonacci search. The procedure is followed through for each point in the interior of the free surface boundary. Should the procedure fail to find the correct zero for f within a specified number of repetitions in increasing or decreasing $y_{imk}$, a message is printed to this effect and the average of the surrounding four y's in the plane of the free surface is used. Also each time it becomes necessary to resort to the Fibonacci search to minimize the absolute value of $f^2$ because a real zero has become nonexistent a message to this effect is printed. It has been observed that after the interior values are well settled and the value x, y, and z on the free surface are also nearly settled that the minimization procedure is called upon only rarely and then only near the stagnation points at the front and rear of the strut.

The boundary condition operator Eq. 60 for x on the free surface is also based on the basic condition, Eq. 77. This equation is obtained by solving Eq. 77 for $x_\phi$ and then integrating the resulting equation by holding $\psi$ and $\psi^*$ constant.

The boundary condition, Eq. 61, for z, however, comes from solving Eq. 20 for $z_{\psi^*}$ and subsequently integrating with $\Phi$ and $\psi$ held constant.

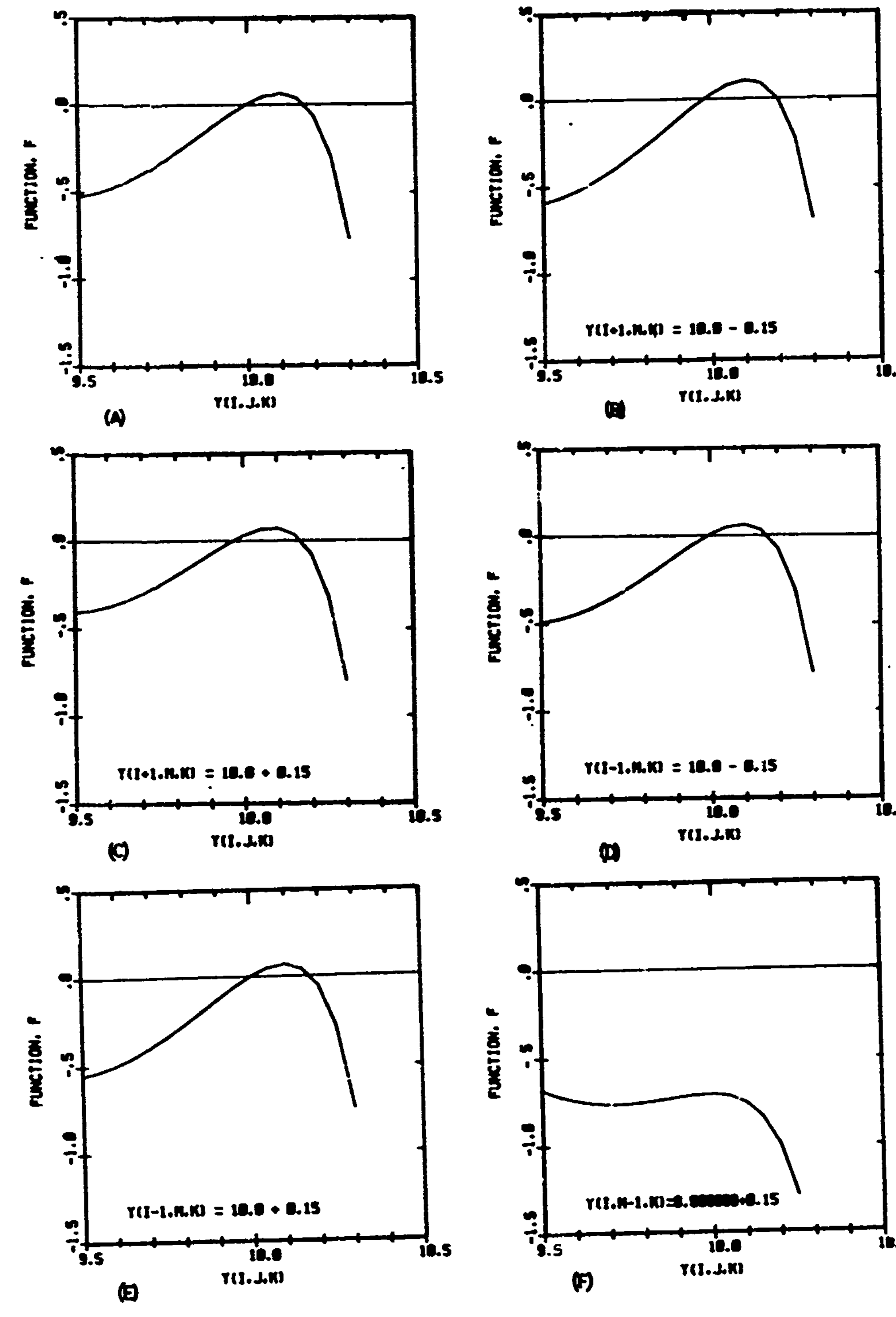


Fig. 3. Variation of the finite difference function given by Eq. 80 over a small range of $y_{imk}$ with no error (A) or a small error at several surrounding grid points (B-Q).

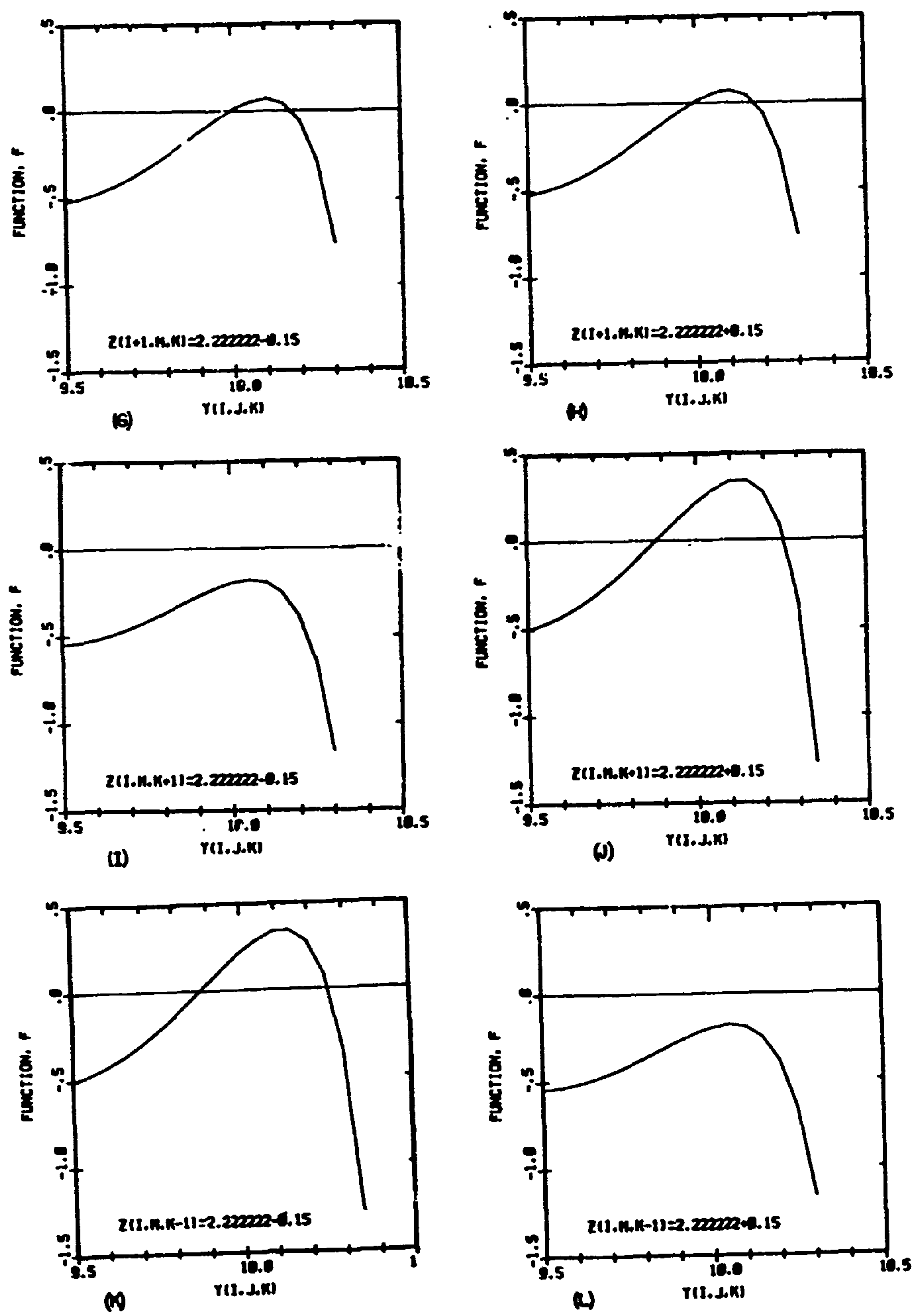


Fig. 3. Continued.

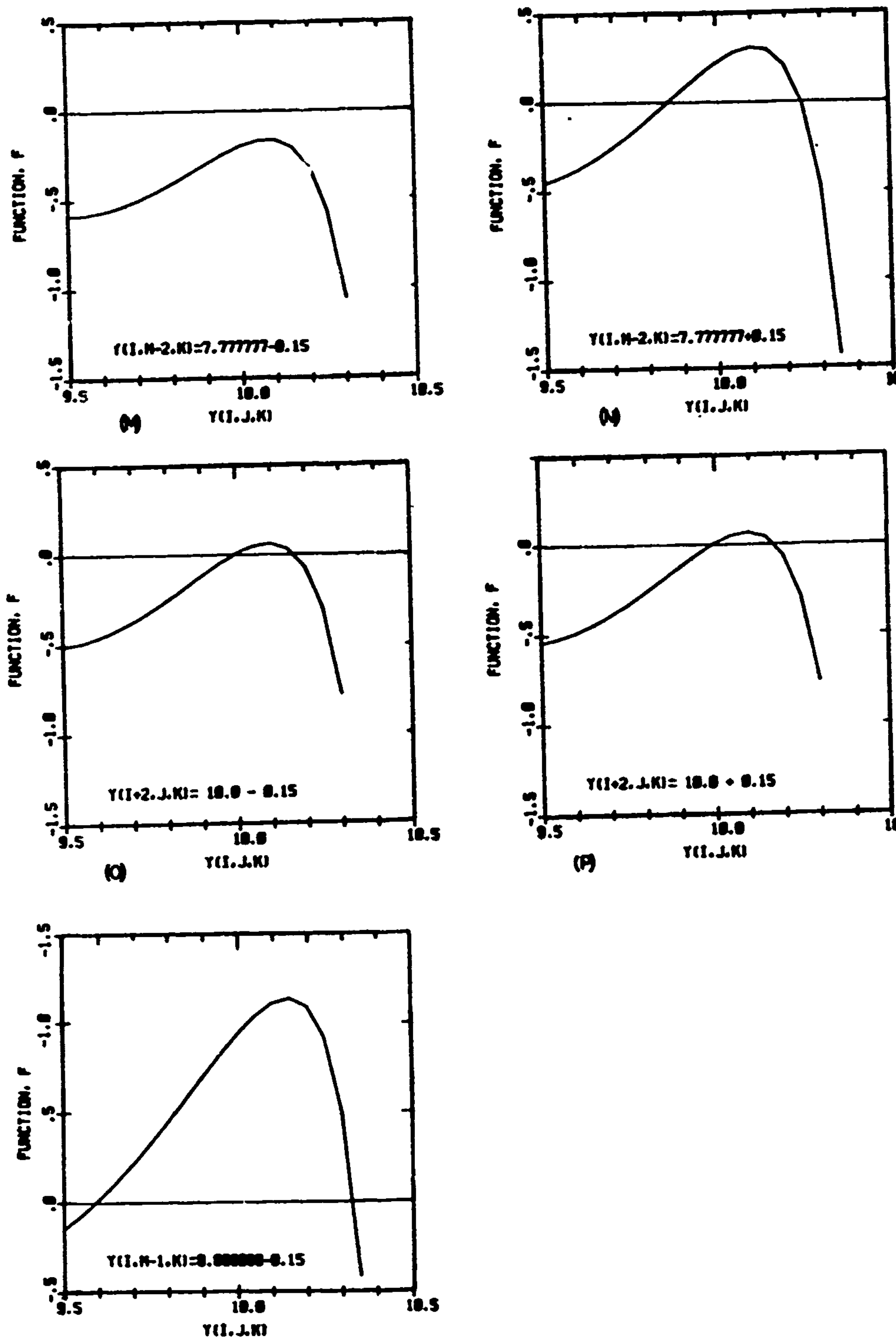


Fig. 3. Continued.

## Computer logic in obtaining solution

The general logic followed in writing the computer program used in obtaining the solution is illustrated in the gross flow chart contained as Fig. 4. While it is not necessary to follow the exact pattern of obtaining tentative solutions given in Fig. 4, it is desirable to provide control, through data input, so that tentative solutions on boundary planes are not necessarily obtained during each cycle. From the above discussion of difficulties associated with obtaining the tentative solution for y on the free surface boundary it is clear that it would not be expedient to call on the subroutine which obtains this tentative solution during the first few cycles, particularly if a rough initialization is used. Also not adjusting those boundary values which are obtained by integration (see Eqs. 49, 60, and 61) until after the interior values have been initially settled contributes to more rapid convergence to the final solution. Consequently specifications are included as part of the input data, which determine during which cycles each of the subroutines will be called to obtain the tentative solution from the boundary condition operators. The present program first obtains all tentative solutions for x, which are called for during that cycle; then it obtains the tentative solution for y before obtaining the tentative solutions for z. Tentative solutions on interior planes are obtained prior to obtaining the tentative solutions for that variable on boundary planes.

The logic followed in obtaining each of the tentative solutions varies slightly dependent upon which variable is involved and whether the plane is interior or a boundary plane. For tentative solutions on interior planes and those boundary planes in which the LSOR method is used to obtain a solution to the boundary condition equation, the flow chart given as Fig. 5 shows the essential logic. On those boundary planes on which the tentative solutions are obtained by numerical line integrations, the logic is such that the required integration is completed a line at a time beginning with a line on or adjacent to an edge, and proceeds until it has been completed for the last line on the opposite edge of the plane.

For use, particularly during earlier cycles, the program provides that the free surface values of y may be smoothed if desired. This smoothing is accomplished by fitting the values of y along i = constant lines (i.e. with k = 1, 2, ... N) on the free surface by least squared regression analysis to an equation of the general form,

$$y_{imk} = b_0 + b_1 k + b_2 k^2 + b_3 \cos (k - NS - 1) \frac{\pi}{N_1} \quad . \quad . (84)$$

in which the b's are the coefficients obtained from the regression analysis. After fitting the y's along each such line to an equation of the form of Eq. 84, they are adjusted to satisfy the equation exactly. The adjustment also includes the y on the two channel walls and the two sides of the strut.

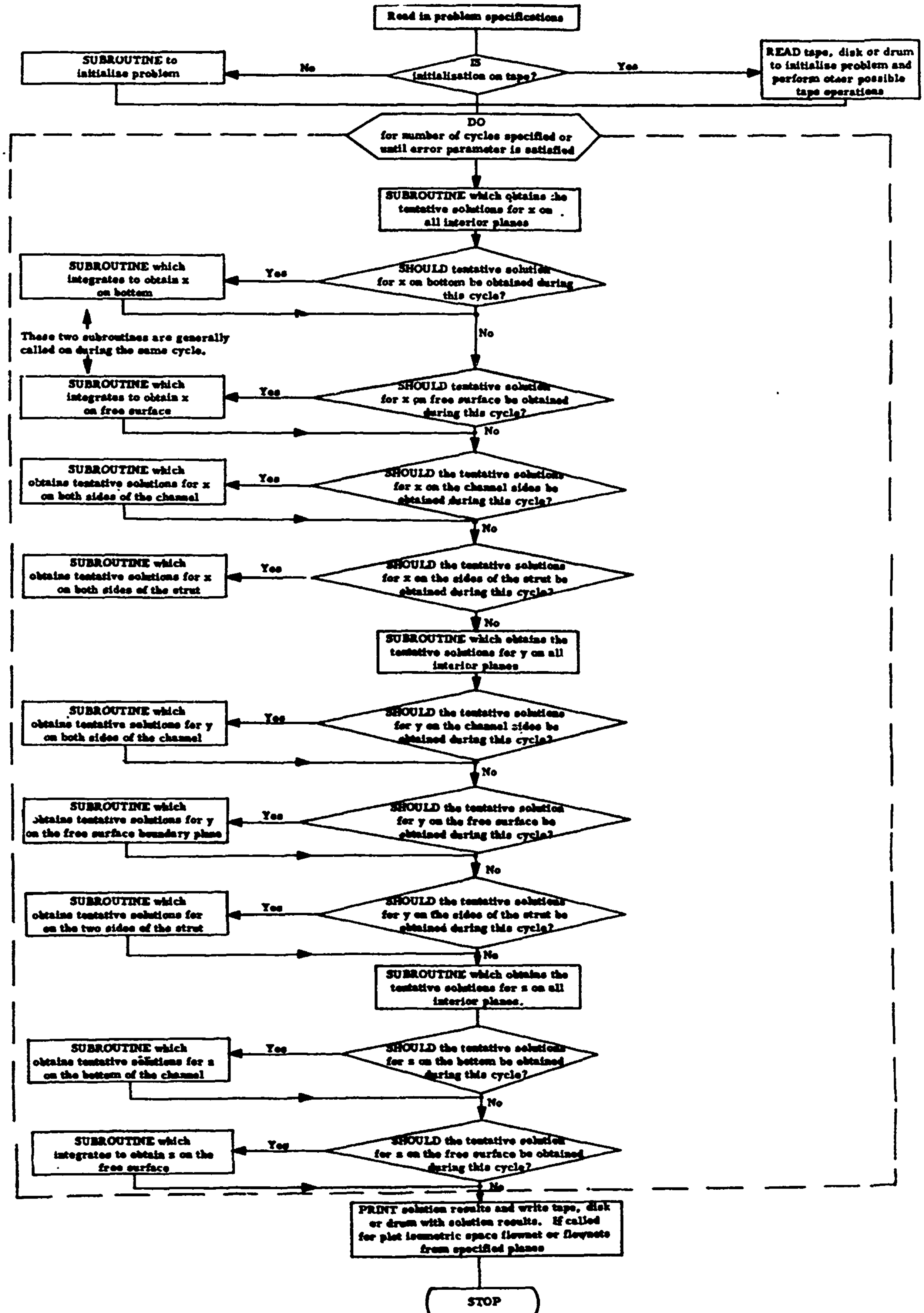


Fig. 4. Flow chart of logic used in obtaining the solution.

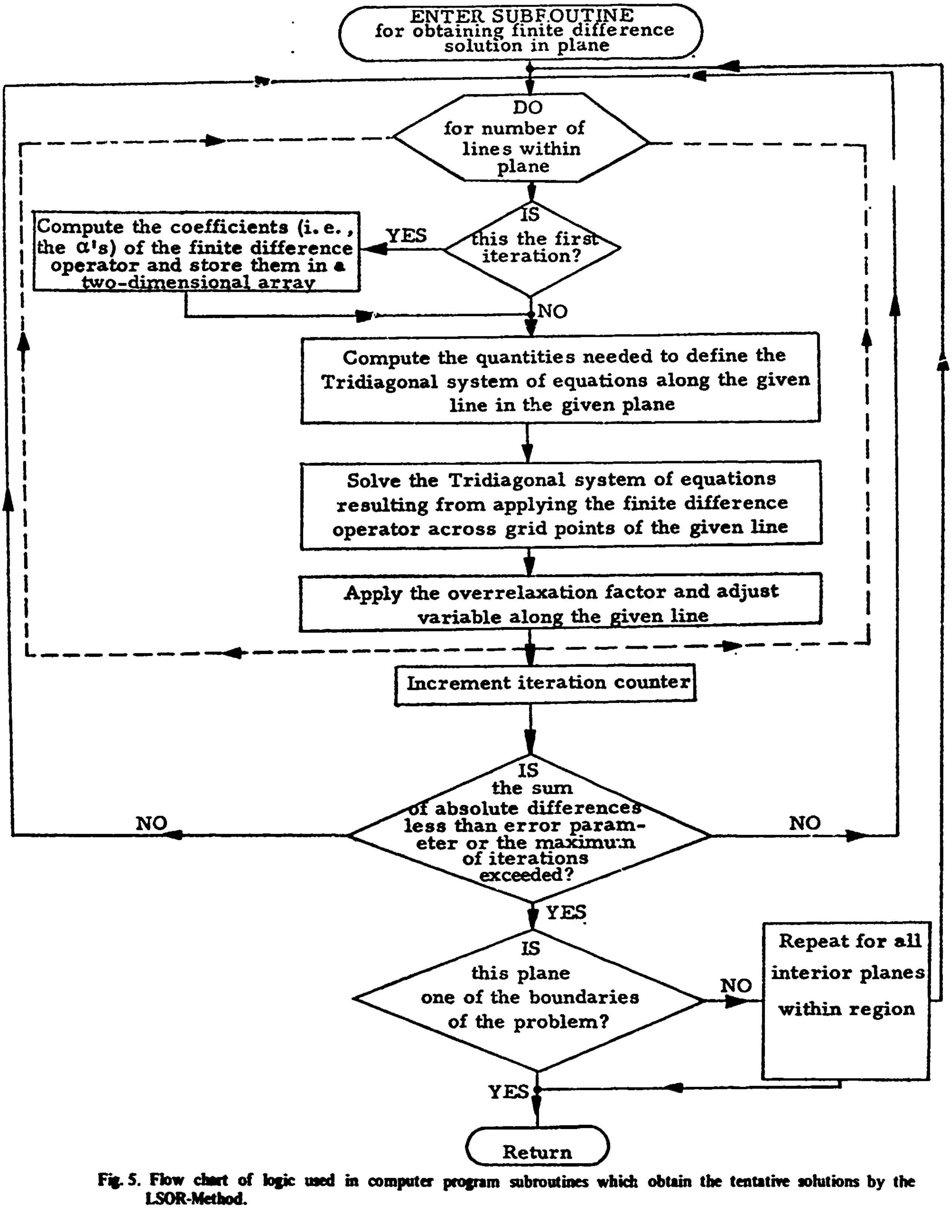


Fig. 5. Flow chart of logic used in computer program subroutines which obtain the tentative solutions by the LSOR-Method.

## SOLUTION RESULTS

The final solution consists of the magnitudes of x, y, and z at all grid points within the $\phi\psi\psi^*$ space used to solve the problem. Consequently the coordinates are given for each intersection of the potential surfaces with all of the orthogonal stream surfaces defined by holding $\psi$ and $\psi^*$ equal to constants. In this form the solution is ideally adapted for presentation as a space flownet. Such a space flownet is constructed by simply connecting all consecutive points defined by the x, y, and z values given at each grid point throughout the $\phi\psi\psi^*$ space by lines in an isometric drawing (or other graphical projections which show depth into the paper as well as the shape within the plane of the paper). The small planes defined by these lines represent the sides of each element of the flownet. The intersection of the $\psi$ and $\psi^*$ constant planes define the streamlines of the flow. The velocity is inversely related to the area of the square formed by the $\psi$ and $\psi^*$ equal constant lines and the distances between consecutive equipotential surfaces as given by combining Eqs. 10, 11, and 12 with Eq. 76 in various ways. (Equations for the velocity and its direction are given later.) That is the velocity is greater in regions in which the volume enclosed within individual cubes (or parallelepiped elements if $\Delta\phi = \Delta\psi = \Delta\psi^*$), of the flownet is smaller than in those regions in which this volume is greater.

While a complete isometric space flownet can readily be obtained by use of a computer driven plotter, the numerous lines resulting therefrom would make visualization of the complete flow difficult. Alternatives are to plot only a few of the flownet lines, or to plot only the flownet lines in key planes. Fig. 6 has been prepared by using this latter type of plot, in which the plane flownets from the top, rear, and right side are given in an isometric projection of the problem.

The more essential specifications used in obtaining the solution, whose flownet is given in Fig. 6, are as follows: (1) The depth of uniform flow upstream from the strut equals 10 feet (2) The number of $\phi\psi^*$ grid planes equals the number of $\phi\psi$ grid planes and consequently the width between channel sides is also 10 feet. (3) The number of $\psi\psi^*$ planes (increments in the $\phi$ direction plus one) was given as 20, resulting in a length from beginning to end of the problem equal to 18.4 feet. (4) The strut was specified 0.6 feet wide at its widest point and it began on the 7th $\psi\psi^*$ plane and ended on the 14th $\psi\psi^*$ plane resulting in a length equal to 6.4 feet. (5) The velocity head in the undistributed uniform flow equals 0.5 feet (H = 10.5 feet), resulting in an upstream velocity equal to 5.675 fps. In solving this problem 2,420 finite difference grid points were used. Since three unknowns must be solved for simultaneously, three times this many finite difference grid points or 7,260, were actually used.

The solution to this problem was obtained in a piecemeal manner as the separate subroutines were debugged, etc. Consequently it is not possible to give the exact amount of computer execution time required for the final solution. With an initialization which is easily generated in a computer program, and using the number of grid points used for this problem, a reasonable estimate of the execution time on an UNIVAC 1108 system is 15 minutes, however.

While an isometric drawing of the space flownets helps in visualizing the complete flow process, more detailed information regarding special features of the flow can be obtained by examining the flow in separate planes within the space. The solution from an inverse formulation is in an ideal form to examine the flow field in separate equipotential planes, i.e. planes defined by $\psi$ and $\psi^*$ axes, or for examining the behavior of the flow in separate planes defined by $\phi\psi$ or $\phi\,\psi^*$ axes. A solution to a three-dimensional problem in the physical space (i.e. in the space defined by the x, y, z cartesian coordinates) would be well adapted for examining details in separate xy planes (i.e. defined by z equal a constant), xz planes or yz planes but would require interpolation to examine the flow field in equipotential planes for instance. On the other hand the results from the inverse solution in the $\phi\,\psi\,\psi^*$ space require interpolation to examine or display the flow in separate planes of the physical space. Thus for example, if one wishes to examine the flow field in an xy plane with z equal to a given constant, it would be necessary to obtain the magnitudes of x and y which define the intersection of the plane flownet lines by interpolation of the x's and y's on the two adjacent inverse planes that contain z values which bracket the specified constant z. Obviously accomplishing this is not difficult; perhaps even less difficult than plotting a flownet given a solution of the potential function in the physical space. However, no flownets from such planes within the physical space are given herein. For boundaries on which either x, y, or z is constant such as the sides, or beginning and end of the channel problem, no interpolation is necessary. The flownets from such boundaries are simultaneously on a plane in which $\phi$, $\psi$ or $\psi^*$ is constant as well as x, y, or z is constant.

Preceding page blank

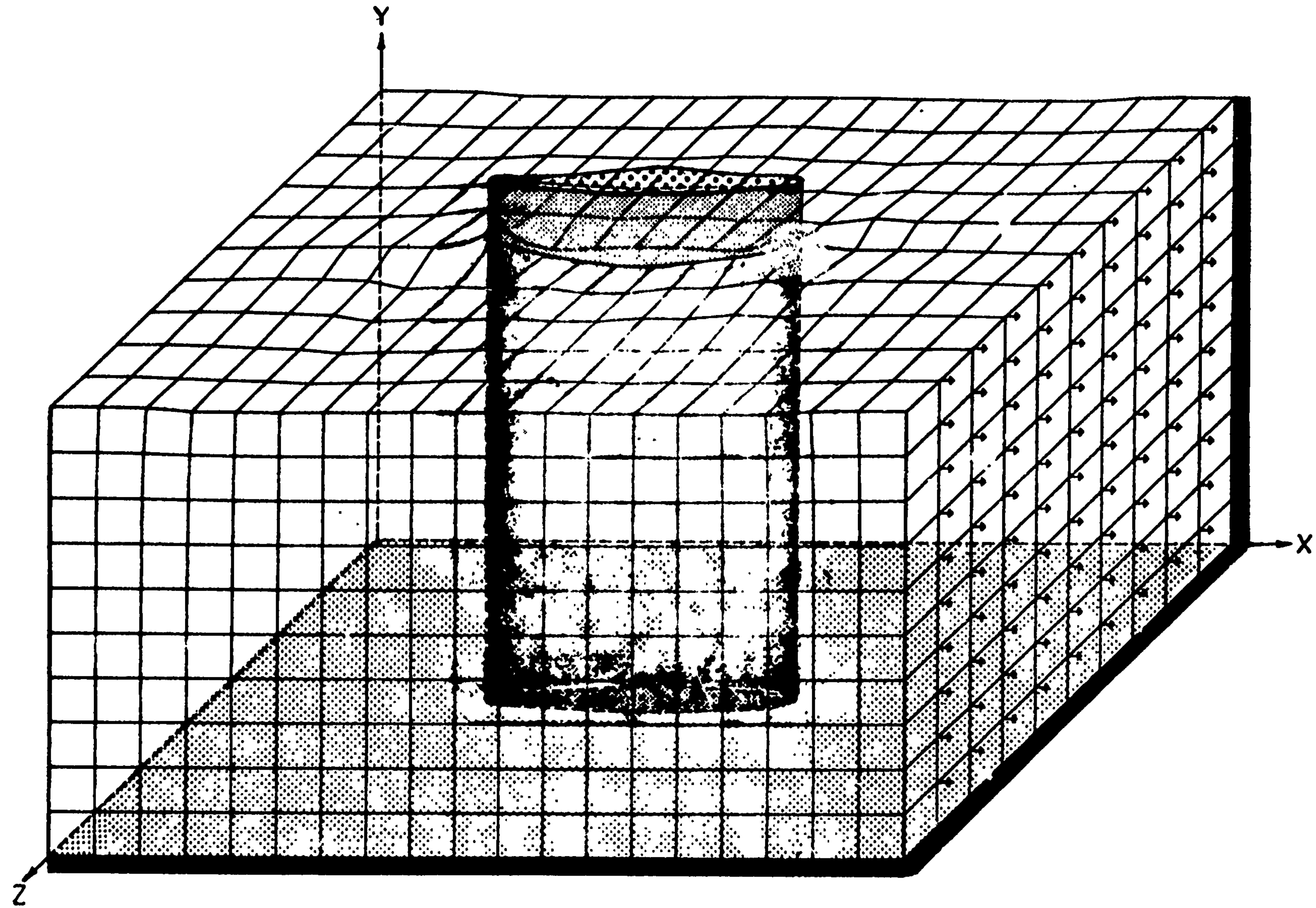


Fig. 6. Isometric drawing of space flownet of a strut in a free surface channel flow.

In general, however, individual plane flownets obtained by holding $\phi$, $\psi$, or $\psi^*$ constant are more useful in visualizing flow patterns than those obtained by holding x, y, or z constant. In understanding plane flownets obtained by holding $\phi$, $\psi$, or $\psi^*$ constant, one needs to interpret the results as projections upon a specified plane. Thus for example if one wished to examine the flow pattern along the sides of the strut, a plane flownet obtained by plotting x and y from the plane with $\psi^*$ equal to the value coincident with the strut, would be a projection of the strut's flow pattern upon a vertical plane parallel to the sides of the channel. Such a flownet is given in Fig. 7.

A plane flownet obtained by plotting the y and z magnitudes of the solution from a $\phi$ equal constant (equipotential plane) is given in Fig. 8. This flownet represents a projection of the flow from the leading edge of the strut unto a vertical plane at right angles to the channel sides.

The plane flownet obtained from the free surface $\psi$ equal constant plane is shown in Fig. 9, in which the x and z magnitudes have been plotted. This flownet can be interpreted as a projection of the free surface flow pattern into a horizontal plane (i.e. a plane parallel to the channel bottom).

The magnitudes of x, y, and z at each intersection of grid planes in the $\phi\psi\psi^*$ space, which constitute the basic solution can readily be used to obtain other quantities of interest about the flow. The local velocity magnitude can be computed from the following finite difference equation derived from Eq. 76.

$$V_{ijk} = \frac{2\Delta\phi\, c_1 V_o}{\left[(x_{i+1jk}-x_{i-1jk})^2+(y_{i+1jk}-y_{i-1jk})^2+(z_{i+1jk}-z_{i-1jk})^2\right]^{1/2}} \quad \ldots\ldots\ldots\ldots (85)$$

in which $c_1 = D/M_1$ is as previously defined, $V_o$ is the undistributed upstream velocity, and $\Delta\phi$ is unity for the solution given herein and can be deleted from the equation.

The direction angles of the velocity vector at any point within the flow space can be obtained by first noting that the first equation of Eqs. 6, 7, and 8 can be written respectively as:

$$V^2 x_\phi = u \quad \ldots\ldots\ldots\ldots (86)$$

$$V^2 y_\phi = -v \quad \ldots\ldots\ldots\ldots (87)$$

$$V^2 z_\phi = w \quad \ldots\ldots\ldots\ldots (88)$$

These equations are obtained by noting that the Jacobian determinant J equals the magnitude of the velocity squared. Since $u = V\cos\alpha$, $v = V\cos\beta$, and $w = V\cos\gamma$ (in which $\alpha$, $\beta$, and $\gamma$ are the angles of the direction cosines for the velocity vector), Eqs. 86, 87, and 88 give

$$\alpha = \cos^{-1}(V x_\phi) \quad \ldots\ldots\ldots (89)$$

$$\beta = \cos^{-1}(V y_\phi) \quad \ldots\ldots\ldots (90)$$

$$\gamma = \cos^{-1}(V z_\phi) \quad \ldots\ldots\ldots (91)$$

The pressure at any point can be computed from Eq. 85 and the Bernoulli equation, i.e.

$$P_{ijk} = \rho g(H - y_{ijk}) - \rho\frac{V_{ijk}^2}{2} \quad \ldots (92)$$

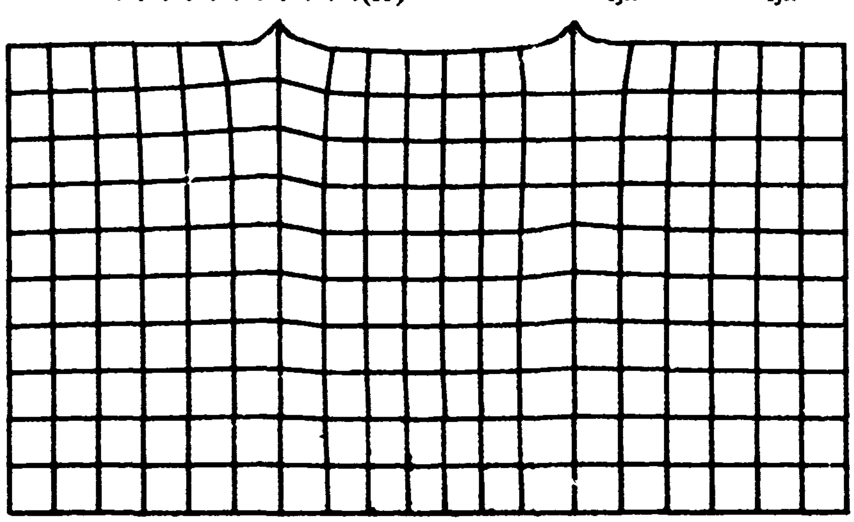

**Fig. 7. Plane flownet from the $\phi\psi$ plane associated with k=6 which coincides with the stream surface $\psi^*$ of the strut obtained by projecting the magnitudes of x and y onto a vertical plane parallel to the channel sides.**

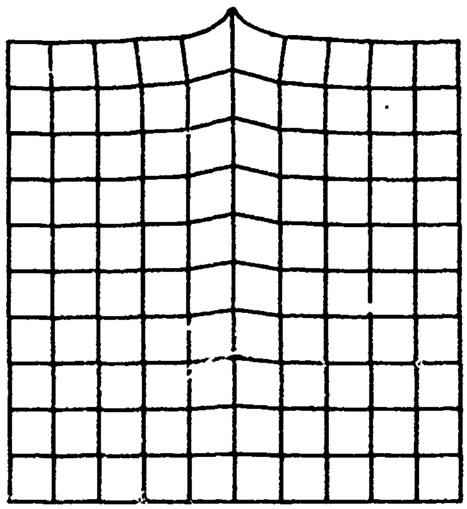

Fig. 8. Plane flownet from the $\psi\psi^*$ plane associated with i=7 which touches the leading edge of the strut and which results from projecting the magnitudes of y and z onto a vertical plane at right angles to the channel sides.

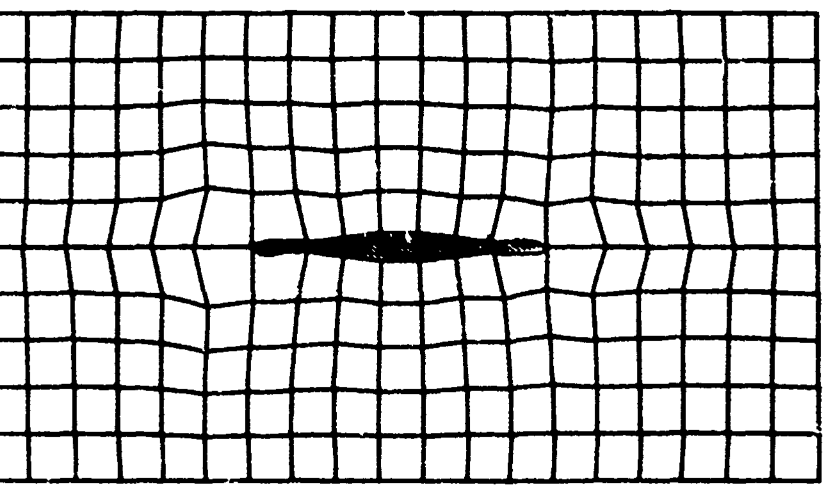

Fig. 9. Plane flownet from the $\phi\psi^*$ plane associated with j=11 which coincides with the free surface obtained by projecting the magnitudes of x and z onto a horizontal plane parallel to the channel bottom.

## CONCLUSIONS AND RECOMMENDATIONS

The use of a mathematical formulation which reverses the usual role of variables shows promise as a valuable tool for numerically solving certain types of three-dimensional potential fluid flow problems. Like most new approaches, however, the merits of the methods need to be further evaluated and improved. The methods and techniques used in this report for solving the inversely formulated space boundary value problem represents an initial approach which is workable, but which will no doubt be streamlined and improved upon with time.

The interchange of the conventional dependent and independent roles played by the variables in a three-dimensional potential fluid flow problem results in advantages similar to those which occur in solving two-dimensional plane and axisymmetric potential fluid flow problems. Perhaps the major advantages are: (1) That the region of the space boundary value problem is a parallelepiped with planes for boundaries, which in the physical plane may be irregular and of unknown position, such as free surfaces or cavity surfaces, and (2) the form of the solution is better adapted for graphical presentation and for computing various items of interest about the flow. These advantages occur at the expense of more complex simultaneous partial differential equations.

In order for the inverse solution method to be readily adaptable and used practically for solving a variety of problems involving free surfaces and cavities, alternate and better schemes or methods are needed for handling boundary conditions resulting from a constant pressure free surface under the influence of gravity. The approach used herein is associated with a number of difficulties which no doubt will become progressively harder to cope with as the complexity of the problem increases. Consequently, a problem with a three-dimensional cavity and free surfaces would represent a difficult undertaking without better methods for handling such free surface boundary conditions. With such improved methods, the inverse formulation should, in fact, provide a practical numerical solution procedure for solving three-dimensional, steady-state, free surface, and cavity potential fluid flow problems.

Even if more satisfactory methods for handling free surface boundary conditions are not developed, the methods still represent a valuable tool for solving three-dimensional problems without free surfaces, particularly if the problem is a design problem instead of an analysis type problem. In a design problem shapes of confining structures are sought which give some desired flow characteristics. The inverse formulation is particularly well adapted for such problems in which the shape of a boundary, which is a stream surface, is part of the solution, resulting from a specification of fluid behavior, but less well adapted if non-plane confining surfaces have specified shapes as in analysis type problems.

# REFERENCES


Ames, W. F. (1965), Nonlinear partial differential equations in engineering. Academic Press, New York.

Cassidy, J. J. (1965), Irrotational flow over spillways of finite height. Journal of the Engineering Mechanics Division, ASCE, Vol. 91, No. EM6, Proc. Paper 4581, December, pp. 155-174.

Forsythe and Wasow (1960), Finite-difference methods for partial differential equations. John Wiley & Sons, Inc., New York.

Jeppson, R. W. (1966), Techniques for solving free-streamline, cavity, jet and seepage problems by finite differences. Technical Report No. 68, Dept. of Civil Engineering, Stanford University, Stanford, California.

Jeppson, R. W. (1968a), Seepage from ditches–solution by finite differences. Journal of the Hydraulics Division, ASCE, Vol. 94, No. HY1, Proc. Paper 5763, January, pp. 259-283.

Jeppson, R. W. (1968b), Seepage through dams in the complex potential plane. Journal of the Irrigation and Drainage Division, ASCE, Vol. 94, No. IR1, Proc. Paper 5835, March, pp. 23-37.

Jeppson, R. W. (1968c), Seepage from channels through layered porous mediums. Water Resources Research, AGU, Vol. 4, No. 4, pp. 435-445.

Jeppson, R. W. (1968d), Axisymmetric seepage through homogeneous and nonhomogeneous porous mediums. Water Resources Research, Vol. 4, No 6, December, pp. 1277, 1288.

Jeppson, R. W. (1969a), Free streamline problems solved by inverse formulation and finite differences. Developments in Mechanics, Vol. 5, Iowa State Univ. Press, Ames, Iowa.

Jeppson, R. W. (1969b), Numerical solutions to free-surface axisymmetric flows. Journal of the Engineering Mechanics Division, ASCE, Vol. 95, No. EM1, Proc. Paper 6381, February, pp. 1-20.

Jeppson, R. W. (1970), Inverse formulation and finite difference solution for flow from a circular orifice. Journal of Fluid Mechanics, Vol. 40, part 1, pp. 215-223.

Jeppson, R. W. and R. W. Nelson. (1970), Inverse formulation and finite difference solution to partially saturated seepage from canals. Soil Science Society of America, Proceedings, Vol. 34, No. 1, January-February, pp. 7-14.

Jeppson, R. W., D. L. Schreiber, G. R. Stephenson, C. W. Johnson, L. M. Cox, and G. A. Schumaker. (1972), Solution of a two-dimensional, steady-state watershed flow system. Proceedings, American Society of Agricultural Engineers.

Mackenroth, E. and G. D. Fisher (1968), Determination of the flow field of an ideal axisymmetric impinging jet. Preprint 31F, Symposium on non linear problems in transport, Part II, Sixty-First Annual Meeting, American Institute of Chemical Engineers, Los Angeles, California, December 1-5.

Markland, E. (1965), Calculation of flow at a free overfall by relaxation method. Proceedings, Institute of Civil Engineers, Vol. 31, May, pp. 71-79.

Nelson, R. W. (1963), Stream functions for three-dimensional flow in heterogeneous porous media. Extract of Publication No. 64, International Association of Scientific Hydrology, Berkeley, California, pp. 290-301.

Thom, A. and C. J. Apelt (1961), Field computations in engineering and physics. D. Van Nostrand Company, Ltd., London.

Varga, R. S. (1962), Matrix iterative analysis. Prentice Hall, Inc., Englewood Cliffs, New Jersey.

Wilde, D. J. and C. S. Beighter (1967), Foundation of optimization. Prentice-Hall, Inc., Englewood Cliffs, N. J.

Yih (1957), Stream functions in three-dimensional flows. LaHouille Blanche, Vol. 12, No. 3, pp. 445-450.